Abnormalities of chromosome 1p in human neuroblastoma tumors and cell lines. Cancer Genet. Cytogenet. **7**:33–42.

16. **Girish, V., and A. Vijayalakshmi.** 2004. Affordable image analysis using NIH Image/ImageJ. Indian J. Cancer **41**:47.
17. **Gonzalez, I., E. J. Andreu, A. Panizo, S. Inoges, A. Fontalba, J. L. Fernandez-Luna, M. Gaboli, L. Sierrasesumaga, S. Martin-Algarra, J. Pardo, F. Prosper, and E. de Alava.** 2004. Imatinib inhibits proliferation of Ewing tumor cells mediated by the stem cell factor/KIT receptor pathway, and sensitizes cells to vincristine and doxorubicin-induced apoptosis. Clin. Cancer Res. **10**:751–761.
18. **Hansen, M. B., S. E. Nielsen, and K. Berg.** 1989. Re-examination and further development of a precise and rapid dye method for measuring cell growth/cell kill. J. Immunol. Methods **119**:203–210.
19. **Hara, S., E. Ishii, S. Tanaka, J. Yokoyama, K. Katsumata, J. Fujimoto, and J. Hata.** 1989. A monoclonal antibody specifically reactive with Ewing's sarcoma. Br J. Cancer **60**:875–879.
20. **Hatori, M., H. Doi, M. Watanabe, H. Sasano, M. Hosaka, S. Kotajima, F. Urano, J. Hata, and S. Kokubun.** 2006. Establishment and characterization of a clonal human extraskeletal Ewing's sarcoma cell line, EES1. Tohoku J. Exp. Med. **210**:221–230.
21. **Homma, C., Y. Kaneko, K. Sekine, S. Hara, J. Hata, and M. Sakurai.** 1989. Establishment and characterization of a small round cell sarcoma cell line, SCCH-196, with t(11;22)(q24;q12). Jpn. J. Cancer Res. **80**:861–865.
22. **Hubert, R. S., I. Vivanco, E. Chen, S. Rastegar, K. Leong, S. C. Mitchell, R. Madraswala, Y. Zhou, J. Kuo, A. B. Raitano, A. Jakobovits, D. C. Saffran, and D. E. Afar.** 1999. STEAP: a prostate-specific cell-surface antigen highly expressed in human prostate tumors. Proc. Natl. Acad. Sci. USA **96**:14523–14528.
23. **Hu-Lieskovan, S., J. Zhang, L. Wu, H. Shimada, D. E. Schofield, and T. J. Triche.** 2005. EWS-FLI1 fusion protein up-regulates critical genes in neural crest development and is responsible for the observed phenotype of Ewing's family of tumors. Cancer Res. **65**:4633–4644.
24. **Im, Y. H., H. T. Kim, C. Lee, D. Poulin, S. Welford, P. H. Sorensen, C. T. Denny, and S. J. Kim.** 2000. EWS-FLI1, EWS-ERG, and EWS-ETV1 oncoproteins of Ewing tumor family all suppress transcription of transforming growth factor beta type II receptor gene. Cancer Res. **60**:1536–1540.
25. **Jones, E. A., S. E. Kinsey, A. English, R. A. Jones, L. Straszynski, D. M. Meredith, A. F. Markham, A. Jack, P. Emery, and D. McGonagle.** 2002. Isolation and characterization of bone marrow multipotential mesenchymal progenitor cells. Arthritis Rheum. **46**:3349–3360.
26. **Khoury, J. D.** 2005. Ewing sarcoma family of tumors. Adv. Anat. Pathol. **12**:212–220.
27. **Kiyokawa, N., Y. Kokai, K. Ishimoto, H. Fujita, J. Fujimoto, and J. I. Hata.** 1990. Characterization of the common acute lymphoblastic leukaemia antigen (CD10) as an activation molecule on mature human B cells. Clin. Exp. Immunol. **79**:322–327.
28. **Konemann, S., T. Bolling, A. Schuck, J. Malath, A. Kolkmeyer, K. Horn, D. Riesenbeck, S. Hesselmann, R. Diallo, J. Vormoor, and N. A. Willich.** 2003. Effect of radiation on Ewing tumour subpopulations characterized on a single-cell level: intracellular cytokine, immunophenotypic, DNA and apoptotic profile. Int. J. Radiat. Biol. **79**:181–192.
29. **Kovar, H., and A. Bernard.** 2006. CD99-positive "Ewing's sarcoma" from mouse bone marrow-derived mesenchymal progenitor cells? Cancer Res. **66**:9786.
30. **Kovar, H., M. Dworzak, S. Strehl, E. Schnell, I. M. Ambros, P. F. Ambros, and H. Gadner.** 1990. Overexpression of the pseudoautosomal gene MIC2 in Ewing's sarcoma and peripheral primitive neuroectodermal tumor. Oncogene **5**:1067–1070.
31. **Lessnick, S. L., C. S. Dacwag, and T. R. Golub.** 2002. The Ewing's sarcoma oncoprotein EWS/FLI induces a p53-dependent growth arrest in primary human fibroblasts. Cancer Cell **1**:393–401.
32. **Lin, P. P., R. I. Brody, A. C. Hamelin, J. E. Bradner, J. H. Healey, and M. Ladanyi.** 1999. Differential transactivation by alternative EWS-FLI1 fusion proteins correlates with clinical heterogeneity in Ewing's sarcoma. Cancer Res. **59**:1428–1432.
33. **Lipinski, M., K. Braham, I. Philip, J. Wiels, T. Philip, C. Goridis, G. M. Lenoir, and T. Tursz.** 1987. Neuroectoderm-associated antigens on Ewing's sarcoma cell lines. Cancer Res. **47**:183–187.
34. **Lochter, A., A. Srebrow, C. J. Sympson, N. Terracio, Z. Werb, and M. J. Bissell.** 1997. Misregulation of stromelysin-1 expression in mouse mammary tumor cells accompanies acquisition of stromelysin-1-dependent invasive properties. J. Biol. Chem. **272**:5007–5015.
35. **May, W. A., A. Arvand, A. D. Thompson, B. S. Braun, M. Wright, and C. T. Denny.** 1997. EWS/FLI1-induced manic fringe renders NIH 3T3 cells tumorigenic. Nat. Genet. **17**:495–497.
36. **May, W. A., S. L. Lessnick, B. S. Braun, M. Klemsz, B. C. Lewis, L. B. Lunsford, R. Hromas, and C. T. Denny.** 1993. The Ewing's sarcoma EWS/FLI-1 fusion gene encodes a more potent transcriptional activator and is a more powerful transforming gene than FLI-1. Mol. Cell. Biol. **13**:7393–7398.
37. **Miyagawa, Y., J. M. Lee, T. Maeda, K. Koga, Y. Kawaguchi, and T. Kusakabe.** 2005. Differential expression of a Bombyx mori AHA1 homologue during spermatogenesis. Insect Mol. Biol. **14**:245–253.
38. **Mori, T., T. Kiyono, H. Imabayashi, Y. Takeda, K. Tsuchiya, S. Miyoshi, H. Makino, K. Matsumoto, H. Saito, S. Ogawa, M. Sakamoto, J. Hata, and A. Umezawa.** 2005. Combination of hTERT and bmi-1, E6, or E7 induces prolongation of the life span of bone marrow stromal cells from an elderly donor without affecting their neurogenic potential. Mol. Cell. Biol. **25**:5183–5195.
39. **Nishimori, H., Y. Sasaki, K. Yoshida, H. Irifune, H. Zembutsu, T. Tanaka, T. Aoyama, T. Hosaka, S. Kawaguchi, T. Wada, J. Hata, J. Toguchida, Y. Nakamura, and T. Tokino.** 2002. The Id2 gene is a novel target of transcriptional activation by EWS-ETS fusion proteins in Ewing family tumors. Oncogene **21**:8302–8309.
40. **Ogose, A., T. Motoyama, T. Hotta, and H. Watanabe.** 1995. In vitro differentiation and proliferation in a newly established human rhabdomyosarcoma cell line. Virchows Arch. **426**:385–391.
41. **Prieur, A., F. Tirode, P. Cohen, and O. Delattre.** 2004. EWS/FLI-1 silencing and gene profiling of Ewing cells reveal downstream oncogenic pathways and a crucial role for repression of insulin-like growth factor binding protein 3. Mol. Cell. Biol. **24**:7275–7283.
42. **Quirici, N., D. Soligo, P. Bossolasco, F. Servida, C. Lumini, and G. L. Deliliers.** 2002. Isolation of bone marrow mesenchymal stem cells by anti-nerve growth factor receptor antibodies. Exp. Hematol. **30**:783–791.
43. **Reyes, M., T. Lund, T. Lenvik, D. Aguiar, L. Koodie, and C. M. Verfaillie.** 2001. Purification and ex vivo expansion of postnatal human marrow mesodermal progenitor cells. Blood **98**:2615–2625.
44. **Reyes, M., and C. M. Verfaillie.** 2001. Characterization of multipotent adult progenitor cells, a subpopulation of mesenchymal stem cells. Ann. N. Y. Acad. Sci. **938**:231–235.
45. **Riggi, N., L. Cironi, P. Provero, M. L. Suva, K. Kaloulis, C. Garcia-Echeverria, F. Hoffmann, A. Trumpp, and I. Stamenkovic.** 2005. Development of Ewing's sarcoma from primary bone marrow-derived mesenchymal progenitor cells. Cancer Res. **65**:11459–11468.
46. **Riggi, N., M. L. Suva, and I. Stamenkovic.** 2006. Ewing's sarcoma-like tumors originate from EWS-FLI-1-expressing mesenchymal progenitor cells. Cancer Res. **66**:9786.
47. **Sekiguchi, M., T. Oota, K. Sakakibara, N. Inui, and G. Fujii.** 1979. Establishment and characterization of a human neuroblastoma cell line in tissue culture. Jpn. J. Exp. Med. **49**:67–83.
48. **Smith, R., L. A. Owen, D. J. Trem, J. S. Wong, J. S. Whangbo, T. R. Golub, and S. L. Lessnick.** 2006. Expression profiling of EWS/FLI identifies NKX2.2 as a critical target gene in Ewing's sarcoma. Cancer Cell **9**:405–416.
49. **Staege, M. S., C. Hutter, I. Neumann, S. Foja, U. E. Hattenhorst, G. Hansen, D. Afar, and S. E. Burdach.** 2004. DNA microarrays reveal relationship of Ewing family tumors to both endothelial and fetal neural crest-derived cells and define novel targets. Cancer Res. **64**:8213–8221.
50. **Takeda, Y., T. Mori, H. Imabayashi, T. Kiyono, S. Gojo, S. Miyoshi, N. Hida, M. Ita, K. Segawa, S. Ogawa, M. Sakamoto, S. Nakamura, and A. Umezawa.** 2004. Can the life span of human marrow stromal cells be prolonged by bmi-1, E6, E7, and/or telomerase without affecting cardiomyogenic differentiation? J. Gene Med. **6**:833–845.
51. **Tondreau, T., N. Meuleman, A. Delforge, M. Dejeneffe, R. Leroy, M. Massy, C. Mortier, D. Bron, and L. Lagneaux.** 2005. Mesenchymal stem cells derived from CD133-positive cells in mobilized peripheral blood and cord blood: proliferation, Oct4 expression, and plasticity. Stem Cells **23**:1105–1112.
52. **Torchia, E. C., S. Jaishankar, and S. J. Baker.** 2003. Ewing tumor fusion proteins block the differentiation of pluripotent marrow stromal cells. Cancer Res. **63**:3464–3468.
53. **Woodbury, D., E. J. Schwarz, D. J. Prockop, and I. B. Black.** 2000. Adult rat and human bone marrow stromal cells differentiate into neurons. J. Neurosci. Res. **61**:364–370.

Int J Hematol (2008) 87:75–77
DOI 10.1007/s12185-007-0007-x

CASE REPORT

Evans syndrome in a patient with Langerhans cell histiocytosis: possible pathogenesis of autoimmunity in LCH

Yoichiro Tsuji · Kazuhiro Kogawa · Kohsuke Imai · Hirokazu Kanegane · Junichiro Fujimoto · Shigeaki Nonoyama

Received: 11 June 2007 / Revised: 25 September 2007 / Accepted: 9 October 2007 / Published online: 27 November 2007

Abstract We report a 1-year-old girl with Evans syndrome coexisting with histologically confirmed Langerhans cell histiocytosis (LCH) affecting the cervical lymph nodes, liver, and spleen. Anti-cardiolipin antibody, anti-SS-A antibody, and anti-SS-B antibody as well as a direct antiglobulin test and platelet-associated IgG were all positive at the onset, and these autoantibodies became negative with the resolution of LCH by chemotherapy. Serum T-helper-2 (Th2) cytokine levels such as those of interleukin (IL)-6 and IL-10 were high whereas those of Th1 cytokines such as IL-2 and interferon-gamma were low at the onset, and this cytokine imbalance was normalized during the resolution of LCH. These results suggest that cytokine imbalance due to LCH led to multiple autoimmune phenomena in the present patient.

Keywords Langerhans cell histiocytosis · Evans syndrome · Cytokines · Hemolytic anemia · ITP · Autoimmune

1 Introduction

Langerhans cell histiocytosis (LCH) is a rare neoplastic disease with a wide clinical spectrum, ranging from a spontaneously regressing solitary lesion of bone to a multisystem, life-threatening disorder [1, 2]. The association of LCH with autoimmune disease is extremely rare, and its coexistence with Evans syndrome has not been reported to date.

Herein, we report a patient with LCH coexisting with autoimmune phenomena including Evans syndrome, and discuss a possible pathogenesis of these rare phenomena.

2 Case report

A 1-year-old female patient was referred to our hospital because of prolonged fever, enlarged cervical lymph nodes, and hepatosplenomegaly. On admission, the bilateral cervical lymph nodes were palpable over a region 10 cm in diameter, and the liver and spleen were palpable 11 and 5 cm below the costal margin, respectively. The white blood cell count was 15.4×10^9/L with 28% bands, 68% segments, 3% lymphocytes, and 1% monocytes. Hemoglobin, the reticulocyte count, and platelet count were 4.4 g/dL, 145×10^9/L, and 48×10^9/L, respectively. Serum LDH was high (473 IU/L), haptoglobin was low (2.4 mg/L), and total bilirubin was normal (0.8 mg/dL). Coagulation studies revealed an international normalized ratio of 1.57 and activated partial thromboplastin time of 49.5 s. Serum IgG was high (1,610 mg/dL). Bone marrow aspiration revealed a normal nuclear cell count (260×10^6/mL), increased megakaryocyte count (9×10^4/mL) and no proliferation of LCH cells. A direct antiglobulin test (IgG and C3) (DAT) was positive and

---

Y. Tsuji (✉) · K. Kogawa · K. Imai · S. Nonoyama
Department of Pediatrics, National Defense Medical College,
3-2 Namiki, Tokorozawa, Saitama 359-0042, Japan
e-mail: ytsuji@ndmc.ac.jp

H. Kanegane
Department of Pediatrics, Faculty of Medicine,
University of Toyama, Toyama, Japan

J. Fujimoto
Division of Developmental Biology and Pathology,
National Research Institute for Child Health
and Development, Tokyo, Japan

platelet-associated IgG (PA-IgG) was high (175.2 ng/10^7 cells, normal value <25). Thus, she was diagnosed with Evans syndrome. In addition, anti-cardiolipin Ab, anti-SS-A Ab, and anti-SS-B Ab were all positive at the disease onset (Table 1). Analysis of lymphocyte subsets revealed marked B cell proliferation (60% of total lymphocytes). As autoimmune lymphoproliferative syndrome (ALPS) was suspected [3], we investigated Fas-mediated apoptosis and TCRαβ+CD4-CD8- T cells (double-negative T cells: DNT). However, Fas-mediated apoptosis was normal and DNT cells did not increase in number (data not shown). As shown in Fig. 1, biopsy of the cervical lymph nodes revealed that S100 protein was positive, Langerin-positive, and CD1a-positive atypical cells were abundant in the specimen, and so the diagnosis of LCH was confirmed. Involved organs were the cervical lymph nodes, liver, and spleen, without any characteristic bone lesion. Several serum cytokines were longitudinally investigated via enzyme immunoassay (Table 1). T-helper-2 (Th2) cytokine levels such as those of interleukin (IL)-6 and IL-10 were high whereas those of Th1 cytokines such as IL-2 and interferon gamma (IFN-γ) were low at the onset.

The patient was treated with induction chemotherapy according to the JLSG-02 protocol, which is almost identical to the JLSG-96 protocol with only minor modification [4], consisting of prednisolone, cytosine arabinoside, and vincristine. Complete remission (CR) was achieved with the resolution of anemia and thrombocytopenia, and all autoantibodies became negative within a few weeks after the beginning of chemotherapy. The normalization of high levels of Th2 cytokines was observed with the resolution of the disease (Table 1). The patient completed maintenance chemotherapy about 1 year ago and remains in CR without treatment.

3 Discussion

LCH with autoimmune disease is rare, but coexisting organ-specific autoimmune disorders such as myasthenia gravis [5] and membranous nephropathy [6] with LCH have been reported in the past. Systemic autoimmune disorder has been reported in only one patient, who had LCH with systemic lupus erythematosus [7]. Hematologic autoimmune disorder has been reported in only one LCH patient with AIHA [8]. Recently, it has been suggested that central diabetes insipidus in LCH, a major complication of this disorder, is caused by vasopressin-cell autoantibody [9]. Thus autoimmunity in LCH may be more common than has been expected. Although Evans syndrome with other autoimmune disorders has been reported in the past [10], coexistence with LCH in this syndrome has not been reported to date. As multiple autoantibodies including DAT and PA-IgG were positive, Evans syndrome was strongly suspected in our LCH patient.

It is well-known that hypercytokinemia plays a central role in the pathogenesis of LCH [11]. In our patient, serum Th2 cytokine levels such as those of IL-6 and IL-10 were high whereas those of Th1 cytokines such as IL-2 and IFN-γ were low at diagnosis, and this cytokine imbalance was normalized with the resolution of LCH. Multiple autoantibodies were initially positive at diagnosis and disappeared

Table 1 Serum autoantibodies, cytokines, and lymphocyte subsets of the patient

	On admission	6th week (at the end of induction)	14th week (during maintenance)	53rd week (at the end of maintenance)	69th week (recent)
DAT	Positive	Negative	Negative	Negative	Negative
PA-IgG (<25)	175.2	18.7		14.1	
ACLAb (<10)	15	<8	<8	<8	12
SS-A Ab (<10.0)	38.8	7.1	<5.0	<5.0	<5.0
SSB Ab (15.0)	15.3	5	<5.0	<5.0	<5.0
IFN-γ (<0.1)	0.2			<0.1	
IL-2 (<0.8)	<0.8			<0.8	
IL-6 (4.0)	180	1.5	0.5	0.3	2.1
IL-10 (<5.0)	86	<2	<2	<2	<2
CD3 (+) cells (%)	34.7	64.1		60.4	
CD4 (+) cells (%)	24	30.8		32.5	
CD8 (+) cells (%)	8.5	30.7		23.3	
CD19 (+) cells (%)	60.7	25.7		33.5	

Numbers of parentheses in the left column represent normal values

DAT direct antiglobulin test, *PA-IgG* platelet-associated IgG, *ACLAb* anti-phospholipid antibody, *SS-A Ab* anti-SS-A antibody, *SS-B Ab* anti-SS-B antibody, *IFN-γ* interferon gamma, *IL* interleukin

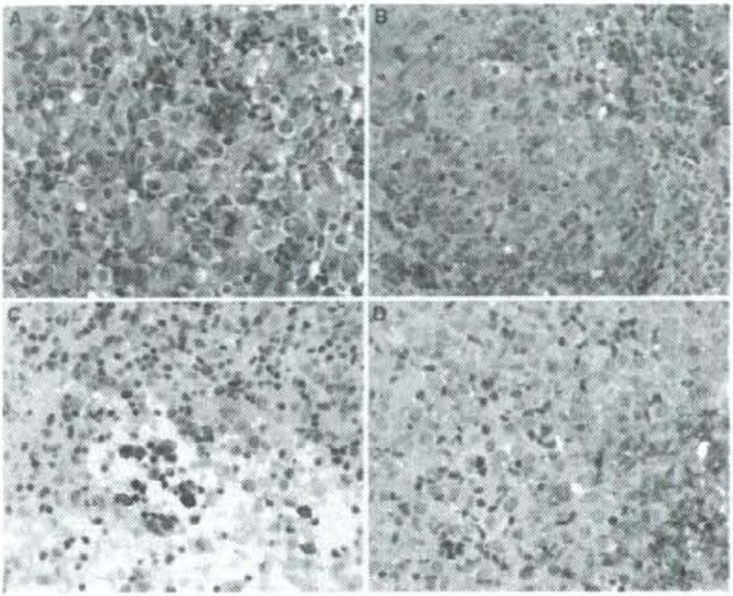

Fig. 1 Biopsy specimen of a cervical lymph node. Atypical, large Langerhans cells are abundant (**a**, hematoxylin-eosin). Immunohistochemical stains revealed that these cells were positive for S-100 (**b**), Langerin (**c**), and CD 1a (**d**)

soon after treatment. These results suggest that the cytokine imbalance had led to the production of multiple autoantibodies in our patient [12].

In summary, cytokine imbalance may have played an important role in the pathogenesis of autoimmunity in our LCH patient. Further investigation is warranted to resolve the pathogenesis of this rare, or may be more common than has been expected, complication in LCH.

Acknowledgments This report was supported by a grant from Kawano Masanori Memorial Foundation for Promotion of Pediatrics.

References

1. Egeler RM, D'Angio GJ. Langerhans cell histiocytosis. J Pediatr. 1995;127(1):1–11.
2. Arico M, Egeler RM. Clinical aspects of Langerhans cell histiocytosis. Hematol Oncol Clin North Am. 1998;12(2):247–58.
3. Teachey DT, Manno CS, Axsom KM, et al. Unmasking Evans syndrome: T-cell phenotype and apoptotic response reveal autoimmune lymphoproliferative syndrome (ALPS). Blood. 2005;105(6):2443–8.
4. Morimoto A, Ikushima S, Kinugawa N, et al. Improved outcome in the treatment of pediatric multifocal Langerhans cell histiocytosis: results from the Japan Langerhans Cell Histiocytosis Study Group-96 protocol study. Cancer. 2006;107(3):613–9.
5. Gilcrease MZ, Rajan B, Ostrowski ML, et al. Localized thymic Langerhans' cell histiocytosis and its relationship with myasthenia gravis. Immunohistochemical, ultrastructural, and cytometric studies. Arch Pathol Lab Med. 1997;121(2):134–8.
6. Rachima CM, Cohen E, Iaina NL, et al. A case of Langerhans'-cell histiocytosis with membranous nephropathy. Am J Kidney Dis. 2004;43(2):e3–9.
7. Robak T, Kordek R, Robak E, et al. Langerhans cell histiocytosis in a patient with systemic lupus erythematosus: a clonal disease responding to treatment with cladribine, and cyclophosphamide. Leuk Lymphoma. 2002;43(10):2041–6.
8. Oliveira MC, Oliveira BM, Murao M, et al. Clinical course of autoimmune hemolytic anemia: an observational study. J Pediatr (Rio J). 2006;82(1):58–62.
9. Maghnie M, Ghirardello S, De Bellis A, et al. Idiopathic central diabetes insipidus in children and young adults is commonly associated with vasopressin-cell antibodies and markers of autoimmunity. Clin Endocrinol (Oxf). 2006;65(4):470–8.
10. Savasan S, Warrier I, Ravindranath Y. The spectrum of Evans' syndrome. Arch Dis Child. 1997;77(3):245–8.
11. Egeler RM, Favara BE, van Meurs M, et al. Differential In situ cytokine profiles of Langerhans-like cells and T cells in Langerhans cell histiocytosis: abundant expression of cytokines relevant to disease and treatment. Blood. 1999;94(12):4195–201.
12. Barcellini W, Clerici G, Montesano R, et al. In vitro quantification of anti-red blood cell antibody production in idiopathic autoimmune haemolytic anaemia: effect of mitogen and cytokine stimulation. Br J Haematol. 2000;111(2):452–60.

Research Article

CD43, but not P-Selectin Glycoprotein Ligand-1, Functions as an E-Selectin Counter-Receptor in Human Pre-B–Cell Leukemia NALL-1

Chizu Nonomura,[1,3] Jiro Kikuchi,[1] Nobutaka Kiyokawa,[4] Hidenori Ozaki,[1] Kanae Mitsunaga,[1]
Hidenobu Ando,[1] Akiko Kanamori,[5] Reiji Kannagi,[5] Junichiro Fujimoto,[4] Kazuo Muroi,[6]
Yusuke Furukawa,[7] and Mitsuru Nakamura[1,2,3]

[1]Cell Regulation Analysis Team, Research Center for Medical Glycoscience, National Institute of Advanced Industrial Science and Technology; [2]Function of Biomolecule, University of Tsukuba, Tsukuba, Japan; [3]Core Research for Evolution Science and Technology of Japan Science and Technology Agency, Kawaguchi, Japan; [4]Department of Developmental Biology, National Research Institute of Child Health and Development, Tokyo, Japan; [5]The Department of Molecular Pathology, Aichi Cancer Center, Chikusa-ku, Nagoya, Japan; and [6]Division of Cell Transplantation and Transfusion and [7]Division of Stem Cell Regulation, Jichi Medical School, Shimotsuke, Tochigi, Japan

Abstract

B-cell precursor acute lymphoblastic leukemia (BCP-ALL/B-precursor ALL) is characterized by a high rate of tissue infiltration. The mechanism of BCP-ALL cell extravasation is not fully understood. In the present study, we have investigated the major carrier of carbohydrate selectin ligands in the BCP-ALL cell line NALL-1 and its possible role in the extravascular infiltration of the leukemic cells. B-precursor ALL cell lines and clinical samples from patients with BCP-ALL essentially exhibited positive flow cytometric reactivity with E-selectin, and the reactivity was significantly diminished by *O*-sialoglycoprotein endopeptidase treatment in NALL-1 cells. B-precursor ALL cell lines adhered well to E-selectin but only very weakly to P-selectin with low-shear-force cell adhesion assay. Although BCP-ALL cell lines did not express the well-known core protein P-selectin glycoprotein ligand-1 (PSGL-1), a major proportion of the carbohydrate selectin ligand was carried by a sialomucin, CD43, in NALL-1 cells. Most clinical samples from patients with BCP-ALL exhibited a PSGL-1$^{neg/low}$/CD43^{high} phenotype. NALL-1 cells rolled well on E-selectin, but knockdown of CD43 on NALL-1 cells resulted in reduced rolling activity on E-selectin. In addition, the CD43 knockdown NALL-1 cells showed decreased tissue engraftment compared with the control cells when introduced into γ-irradiated immunodeficient mice. These results strongly suggest that CD43 but not PSGL-1 plays an important role in the extravascular infiltration of NALL-1 cells and that the degree of tissue engraftment of B-precursor ALL cells may be controlled by manipulating CD43 expression. [Cancer Res 2008;68(3):790–9]

Introduction

Infiltrating ability is one of the most important characteristics of leukemia cells (1, 2). After infiltration and engraftment, a proportion of leukemia cells is thought to be maintained in microenvironmental niches and escape the effects of anticancer drugs (3, 4). A small population of leukemia cells is known for their ability to transplant disease to a recipient and is experimentally called leukemic stem cells (3). They also home, engraft, and are maintained in their supportive microenvironmental niches (3, 5–7). Therefore, inhibition of leukemia cell infiltration and engraftment may improve the treatment outcome of patients with leukemia.

B-cell precursor acute lymphoblastic leukemia (BCP-ALL/B-precursor ALL) is the most common childhood malignancy and the second most common acute leukemia in adults (2). Eighty percent and 76% of ALLs are of B-lineage in childhood and adulthood, respectively, 95% of B-lineage acute leukemias are BCP-ALLs in adulthood, and B-precursor ALL consists of pro-B ALL, common ALL, and pre-B ALL (2). Although the remission rate is relatively high in patients with BCP-ALL, the disease often relapses in the central nervous system (CNS) and peripheral organs (2). This is in part attributable to the ability of BCP-ALL cells to infiltrate and engraft into the liver, spleen, and CNS. Hepatomegaly, splenomegaly, and lymphadenopathy are found in about 69% to 86% of patients at the first medical examination and hepatosplenomegaly per se is one of the risk factors (1, 8). Infiltration to the CNS is found in <10% of patient at the first examination but such patients are also in a high-risk group (1). In this context, manipulating the tissue infiltration of BCP-ALL cells could be important.

Leukocytes emigrate from blood into peripheral tissues through the sequential interactions of selectins with their ligands, chemokines with their receptors, and integrins with their ligands (9–11). Precursor-B cells and BCP-ALL cell lines are known to express selectin ligands, chemokine receptors, and integrins, and these adhesion molecules may play important roles in cell migration. Carbohydrate selectin ligands are expressed in BCP leukemia cells and the down-regulation of their expression influences tissue infiltration (12). CXCR4, a receptor for stromal cell-derived factor-1, is involved in the localization of BCP-ALL cells and precursor-B cells within the bone marrow (BM) stromal layer (13, 14). β_1/β_2 integrins are expressed in BCP-ALL cells (15) and involved in the intercellular association between BCP-ALL cells and BM stromas (16). Thus, it is important to reveal which adhesion molecules are expressed and how their expression is regulated to understand the mechanisms of leukemia cell homing and engraftment.

We reported previously that BCP-ALL cell lines express a sialyl-Lewis-X (sLe^{X})-related carbohydrate structure, the amount of

---

Requests for reprints: Mitsuru Nakamura, Cell Regulation Analysis Team, Research Center for Medical Glycoscience, National Institute of Advanced Industrial Science and Technology, Central-2, 1-1-1 Umezono, Tsukuba 305-8568, Japan. Phone: 81-29-861-2745; Fax: 81-29-861-2744; E-mail: owl.nakamura@aist.go.jp.

doi:10.1158/0008-5472.CAN-07-1459

which is regulated by core 2 β1,6-*N*-acetylglucosaminyltransferase-1 (C2GnT1) during differentiation (17–19). Another important glycosyltransferase, α1,3-fucosyltransferase-VII, was involved in sLe^X biosynthesis in BCP-ALL cells but did not exhibit significant change during pre-B-cell differentiation (17, 18). Knockdown of C2GnT1 in a B-precursor ALL cell line resulted in a reduction in leukemic cell tissue migration using mouse model (12). Moreover, the sLe^X-related structure was mainly located on an *O*-glycosylated protein (17, 18). On treatment of BCP-ALL cells with an *O*-sialoglycoprotein–specific endopeptidase, leukemic cell migration reduced *in vivo* (12).

For the selectin counter-receptor in leukocytes, P-selectin glycoprotein ligand-1 (PSGL-1) has been identified as the major ligand of P-selectin and E-selectin (20–22). As for BCP-ALL cells, the major carrier of selectin ligands is expected to be a sialomucin (12, 17, 18) but has yet to be identified. In the present study, we show that CD43 functions as an E-selectin counter-receptor in a BCP-ALL cell line. BCP-ALL cells exhibited a PSGL-1$^{neg/low}$/CD43^{high} phenotype. Although BCP leukemia NALL-1 cells rolled well on E-selectin, knockdown of CD43 resulted in the inhibition of this rolling. In addition, CD43 knockdown led to decreased tissue engraftment in a mouse model. These results suggest that CD43 but not PSGL-1 is a selectin counter-receptor in BCP leukemia NALL-1 cells and plays an important role in their peripheral tissue infiltration and that manipulation of CD43 expression may control the tissue infiltration and engraftment of leukemic cells.

Materials and Methods

Cells and cell culture. The human BCP-ALL cell lines NALL-1, Nalm-6, Nalm-16, Nalm-20, KOPN-8, KOPN-K, BV-173, and LAZ221, the human Burkitt's lymphoma cell line Raji, and the human promyelocytic leukemia cell line HL60 were maintained in RPMI 1640 (Sigma-Aldrich). 293FT cells (Invitrogen) were cultured in DMEM. Chinese hamster ovary (CHO) cells overexpressing human E-selectin (CHO-E cells) were maintained in α-MEM. Cells were cultured at 37°C in 5% CO$_2$, and the culture medium was supplemented with 10% fetal bovine serum (FBS), 100 units/mL penicillin, and 100 μg/mL streptomycin. BM cells from patients with BCP-ALL were obtained after informed consent and used according to procedures approved by our Institutional Review Boards.

Flow cytometry and cell sorting. Flow cytometry and cell sorting were carried out using FACSAria (BD Biosciences). E-selectin/P-selectin binding was detected using recombinant E-selectin and P-selectin–human immunoglobulin chimeras (E-selectin/Ig and P-selectin/Ig; R&D Systems) in the presence of 1 mmol/L CaCl$_2$ or 10 mmol/L EDTA. R-phycoerythrin (R-PE)-conjugated anti-human Ig (Jackson ImmunoResearch Laboratories) was used as the secondary antibody. The expression of cell surface sialomucins was detected with FITC-conjugated anti-human CD43 (1G10; BD Biosciences), R-PE–conjugated anti-human CD43 (DF-T1; Serotec), or R-PE–conjugated anti-human PSGL-1 antibody (KPL-1; BD Biosciences). The expression of other cell surface molecules was examined using monoclonal antibodies (mAb) for integrin β_1 (CD28; DF5; Chemicon International), VLA4α (CD49d; SG/73; Seikagaku), integrin β_2 (CD18; 6.7; BD Biosciences), LFA1α (CD11a; B-B15; T Cell Diagnostics), ICAM-1 (CD54; VF27; T Cell Diagnostics), L-selectin (CD62L; MHL1; Seikagaku), and CD44 (A3D8; Sigma-Aldrich). The detection was carried out using an indirect immunofluorescence method with secondary anti-mouse Ig antibody conjugated with R-PE. The expression of chemokine receptors was detected with R-PE–conjugated mAbs for CCR7 and CXCR5 (for spleen; R&D Systems), CCR6 and CXCR3 (for liver; R&D Systems), and CXCR4 (12G5 for BM; BD Biosciences).

Low-shear-force cell adhesion assay. This assay was carried out essentially as described (23), except for the cell-labeling procedure. Briefly, multiplate wells were coated with E-selectin/P-selectin/Ig or control IgG at a final concentration of 5 μg/mL overnight at 4°C and washed thrice with PBS. Cells were labeled with 2′,7′-bis-(2-carboxyethyl)-5-(and-6)-carboxyfluorescein, acetoxymethyl ester (BCECF-AM; Molecular Probes), washed with PBS thrice, added to wells coated with selectin/Ig, and incubated for 30 min at 37°C on a shaking incubator at 60 rpm to maintain shear stress conditions. Nonadherent cells were washed off thrice with TBS-CaCl$_2$ or TBS-EDTA. The adherent cells were lysed in 0.5% NP40, and fluorescence intensity was measured with an Arvo SX 1420 multilabel counter (Wallac). The number of cells was calculated from the fluorescence intensity based on a standard curve prepared simultaneously using BCECF-AM–labeled NALL-1 cells.

Inhibition of *O*-glycan biosynthesis and enzymatic breakdown of sialomucins. For the enzymatic breakdown of cell surface sialomucins, cells were cultured for 3 days with daily additions of fresh *O*-sialoglycoprotein endopeptidase (OSGPEP'ase; Cederlane). The sensitivity of the major selectin ligand carrier protein to OSGPEP'ase was also examined by treating cell lysates with the endopeptidase for 3 h at 37°C.

Western and selectin blot analyses. Western blotting was performed as described (18) using mAbs for sLe^X (CSLEX1; HB85800; American Type Culture Collection), CD43 [DF-T1 (Sigma-Aldrich) and MEM59 (Monosan)], PSGL-1 (KPL-1), or β-actin (AC-15; Abcam plc). Cell lysates were subjected to a 5.0% or 7.5% SDS-PAGE under reducing or nonreducing conditions and transferred to polyvinylidene difluoride membranes (Bio-Rad Laboratories). After blocking, the membranes were incubated with the primary antibody overnight at 4°C. The blots were incubated with a secondary goat anti-mouse IgM or IgG antibody conjugated with horseradish peroxidase (HRP) for 2 h at room temperature. Signals were visualized with a chemiluminescent substrate (GE Healthcare Bioscience). Selectin blotting was performed essentially as above using E-selectin/Ig, biotin-conjugated anti-human Ig, and HRP-conjugated streptavidin.

Immunoprecipitation. Total cell lysate was precleared using protein L-Sepharose (Pierce Biotechnology) or protein G-Sepharose (Sigma-Aldrich) at 4°C with 1 h of agitation. For each immunoprecipitation reaction, 400 μL of cleared lysate were incubated with 50 μL of CSLEX1 or MEM59 at 4°C overnight, and then 50 μL of protein L-Sepharose or protein G-Sepharose were added and incubated for an additional 1 h. Immunocomplexes were precipitated by centrifugation, washed thrice with radioimmunoprecipitation assay (RIPA) buffer [25 mmol/L Tris-HCl (pH 8.0), 150 mmol/L NaCl, 1% NP40, protease inhibitor mixture (Complete Mini EDTA-free, Roche Diagnostics)], and finally resuspended in the sample buffer and boiled for 5 min. The released proteins were examined by Western blotting.

Biotinylation of cell surface proteins and selectin pull-down. Surface proteins were labeled with biotin using a Sulfo-NHS-LC-Biotin kit according to the manufacturer's instructions (Pierce Biotechnology). Cells were washed thrice with PBS containing 100 mmol/L glycine and lysed with RIPA buffer containing 1 mmol/L CaCl$_2$. The lysate was cleared by centrifugation and the supernatant was pretreated with protein G-Sepharose. After centrifugation, the supernatant was incubated overnight at 4°C with recombinant human E-selectin/Ig and then for another 2 h at 4°C with protein G-Sepharose. After centrifugation, the pellets were directly analyzed by SDS-PAGE or resuspended in immunoprecipitation buffer containing 10 mmol/L EDTA, and the eluted proteins were immunoprecipitated with anti-CD43 and protein G-Sepharose followed by SDS-PAGE. Biotinylated proteins were visualized using streptavidin-HRP and chemiluminescence substrate (GE Healthcare Bioscience).

Gene silencing by lentiviral RNA interference. Short hairpin/short interfering RNA (shRNA/siRNA; refs. 12, 24) was introduced into NALL-1 cells to down-regulate *CD43* expression by the shRNA lentivirus system. Oligonucleotides were chemically synthesized, annealed, terminally phosphorylated, and inserted into the vector pLL3.7. The oligonucleotides containing siRNA target sequences were 5′-tgatgtacaccacttcaataacgcttcctgtcacgttattgaagtggtgtacatcttttttc-3′ (forward #1), 5′-tcgagaaaaaagatgtacaccacttcaataacgtgacaggaagcgttattgaagtggtgtacatca-3′ (reverse #1), 5′-tgagcctttggtctctactattcaagagatagtagagaccaaaggctcttttttc-3′ (forward #2), and 5′-tcgagaaaaaagagcctttggtctctactatctcttgaatagtagagaccaaaggctca-3′ (reverse #2) and those containing a scrambled control sequence of #1 were 5′-tgcaatattacatatacgccttcaagagaggcgtatatgtaatattgcttttttc-3′ (forward) and

5′-tcgagaaaaaagcaatattacatatacgcctctcttgaaggcgtatatgtaatattgca-3′ (reverse); nucleotide sequences corresponding to the siRNA are underlined. The resulting plasmids or the parental pLL3.7, along with lentiviral packaging mix (ViraPower, Invitrogen), were transfected into 293FT cells (Invitrogen) to produce recombinant lentivirus, and the NALL-1 cells were infected with the virus. Enhanced green fluorescent protein–positive cells were purified by FACSAria as shRNA-transfected cell populations (NALL-1siCD43#1, NALL-1siCD43#2, NALL-1scrambled, and NALL-1pLL3.7, respectively).

Gene expression analysis. *CD43* and *β-actin* transcripts were detected by the real-time PCR method. The primer set and probe for *CD43* were as follows: forward, 5′-cacttcaataacaagtgaccctaagg-3′; reverse, 5′-tggtaggttgttggctcaggta-3′; probe, 5′-FAM-ccagacctcagccctacctccctcaa-TAMRA-3′. Those for *matrix metalloproteinase 2* (*MMP2*), *MMP9*, and *β-actin* were purchased from Applied Biosystems. PCR products were continuously measured with a Prism 7000 (Applied Biosystems).

Rolling assay. The rolling assay was performed using a flow chamber (GlycoTech) and CHO-E cells as described (25, 26) with a slight modification. The cells were grown on fibronectin-coated dishes and served as a rolling substrate. The flow chamber for rolling assays was mounted on the stage of an inverted microscope (model IX71, Olympus Products). Test cells were introduced into the flow chamber at a concentration of 5×10^5/mL in RPMI 1640 supplemented with 10% FBS and 1 mmol/L $CaCl_2$. Shear stress in the flow chamber was controlled using a syringe pump (Harvard Apparatus). The number of rolling cells and rolling velocity was measured by tracking an individual cell frame by frame (Digimo).

Migration of BCP-ALL cells *in vivo* model. Test cells, NALL-1siCD43#1 or NALL-1scrambled, were labeled with tetramethylrhodamine-5-isothicyanate (TRITC; Molecular Probes) and control NALL-1 parental cells were labeled with carboxyfluorescein diacetate succinimidyl ester (CFSE; Molecular Probes; ref. 27). Both cells were mixed (1:1) and i.v. injected (1×10^8/mouse) into sublethally γ-irradiated (3.3 Gy) nonobese diabetic/severe combined immunodeficient (NOD/SCID) mice (28). Mice were killed 6 and 24 h after injection, and the spleen, liver, and peripheral blood were sampled. The tissues were minced and filtrated to obtain single-cell suspensions. A BM cell suspension was also prepared from a pair of femurs and tibiae. TRITC-labeled test cells were counted as the engrafted cells in the peripheral organs. The number of test cells injected was normalized using CFSE-labeled control cells at each point of assay. All animal experiments were carried out with approval from our Institutional Review Boards.

Assay for gelatinase activity. Gelatin zymography was used to detect gelatinase activity as described elsewhere (29).

Statistical analysis. The significance of differences between the control and experimental groups was determined with Student's *t* test.

Results

Human BCP-ALL cell lines express selectin ligands. NALL-1 was first reported as a "null" cell line (30) but proved to have B-precursor cell markers (31). The cells are thought to inherit the typical characteristics of common ALL, the major population of BCP-ALLs [terminal deoxynucleotidyl transferase positive (TdT^+)/$CD19^+$/$CD10^+$/sIg^-; ref. 2]. So we chose NALL-1 in this study as a model of BCP-ALL. We first carried out flow cytometry using E-selectin/Ig and P-selectin/Ig to test whether the cells express selectin ligands. As shown in Fig. 1*A* (*top*), NALL-1 cells were positively stained with E-selectin/P-selectin in the presence of $CaCl_2$. Other TdT^+/$CD19^+$/$CD10^+$/sIg^- BCP-ALL cell lines, Nalm-6, Nalm-16, Nalm-20, KOPN-8, KOPN-K, BV-173, and LAZ221, were also essentially positive for E-selectin and/or P-selectin (Table 1A, left two columns). These results suggest that BCP-ALL cells express selectin ligands.

Clinical BCP-ALL samples express selectin ligand. To investigate whether BCP-ALL cell lines inherit the immunophenotype of primary B-precursor ALL cells, we performed a flow cytometric analysis of BM-derived leukemia cells from 13 patients with BCP-ALL. The cells were stained with E-selectin/P-selectin (Table 1B, left two columns). This suggests that BCP-ALL cell lines inherit the immunophenotype of primary B-precursor ALL cells as far as the expression of selectin ligands is concerned.

BCP-ALL cell lines functionally adhere to E-selectin but only very weakly to P-selectin. Although NALL-1 cells bound to both E-selectin/P-selectin in the flow cytometric analysis, it is not clear whether the binding is actually functional. To evaluate the function of selectin ligands on NALL-1 cells, we carried out a low-shear-force cell adhesion assay. The data clearly showed that NALL-1 cells functionally adhere to E-selectin but adhere very poorly to P-selectin (Fig. 1*B*, *white columns*). HL60 cells adhered to both selectins (*gray columns*). The other BCP-ALL cell lines, Nalm-6, Nalm-16, Nalm-20, KOPN-8, KOPN-K, BV-173, and LAZ221, were also tested for functional reactivity with E-selectin/P-selectin. These cells also showed a preference for E-selectin (Fig. 1*C*). The results suggest that the data from flow cytometric analyses should be carefully interpreted and that E-selectin rather than P-selectin is the functional partner of BCP-ALL cell lines.

Identification of the major selectin ligand carrier protein as a sialomucin. Our previous findings suggest that carbohydrate selectin ligands on BCP-ALL cell lines are mainly carried by an *O*-glycosylated protein and that the contribution of *N*-glycans or glycosphingolipids may not be significant (12, 17–19). To test whether the selectin ligand on NALL-1 cells was sensitive to sialomucin-specific endopeptidase, flow cytometry was first carried out using NALL-1 cells treated with OSGPEP'ase for 3 days. As exhibited in Fig. 1*A* (*bottom left*), the reactivity with E-selectin decreased significantly. This suggests that the E-selectin ligand on NALL-1 cells is carried by sialomucin(s). On the other hand, the effect of OSGPEP'ase on P-selectin reactivity was minimal (*bottom right*). This suggests that the P-selectin ligand on NALL-1 cells is carried by some OSGPEP'ase-resistant glycoconjugate(s) or the reactivity with P-selectin detected by flow cytometry is not functional in NALL-1 cells. In the subsequent analyses of this study, we focused on the identification and function(s) of the OSGPEP'ase-sensitive E-selectin ligand on BCP-ALL cells.

Subsequently, we performed an immunoblot analysis of NALL-1 cell lysate to detect the E-selectin counter-receptor(s). As shown in Fig. 1*D* (*lane 1*), we observed one major sLe^X-carrying protein. This major sLe^X carrier had an apparent molecular mass of ~135 kDa on 7.5% SDS-PAGE (*lane 5*) and was designated gp135. To identify gp135 as a sialomucin, cell lysates were treated with OSGPEP'ase and analyzed using immunoblotting with anti-sLe^X mAb. As shown in *lane 2*, gp135 was OSGPEP'ase sensitive; the signal became faint after the treatment. As a positive control for the enzyme treatment, the blot was reprobed with an anti-CD43 mAb, DF-T1. CD43 was sensitive to OSGPEP'ase (*lane 4*). To our surprise, CD43 was identical or very similar in size to gp135 (*lanes 1* and *3*). To test whether gp135 was an E-selectin ligand carrier, we performed blotting of NALL-1 cell lysate. With the blotting, a main band (~135 kDa) was detected along with a minor signal (~180 kDa; *lane 7*). The intensity of the major gp135 signal was reduced on pretreatment with OSGPEP'ase, whereas the minor signal did not decrease (*lane 8*). With OSGPEP'ase treatment, the signal detected with the anti-sLe^X and anti-CD43 mAbs disappeared completely (*lanes 6* and *10*). The size of gp135 was very close to that of CD43 (*lanes 5*, *7*, and *9*). These results suggest that gp135 is the major

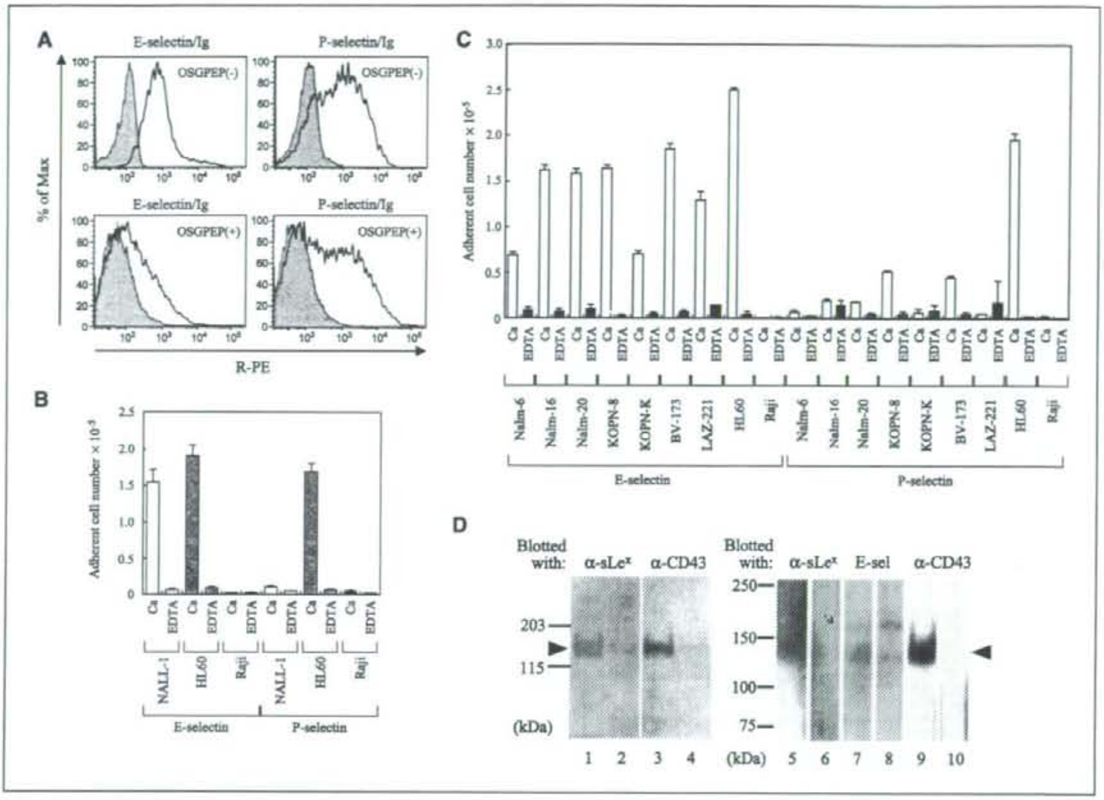

Figure 1. Reactivity with selectins on NALL-1 cells, low-shear-force cell adhesion assays of BCP-ALL cell lines, and analysis of the major E-selectin counter-receptor on NALL-1 cells. *A,* reactivity with E-selectin/P-selectin on NALL-1 cells pretreated with or without OSGPEP'ase. Cells were cultured in the presence or absence of OSGPEP'ase for 3 d, harvested, and subjected to flow cytometry. *Solid line,* the detection was carried out with human recombinant E-selectin or P-selectin in the presence of $CaCl_2$. *Gray shaded area,* reactivity in the presence of EDTA. *Top,* in the absence of OSGPEP'ase; *bottom,* in the presence of OSGPEP'ase. *B,* low-shear-force cell adhesion analysis of NALL-1 cells. Cells were labeled with BCECF-AM and incubated at 37°C for 30 min under low shear stress in well coated with selectin/Ig chimeric proteins. *White columns,* NALL-1; *gray columns,* HL60; *black columns,* Raji. *Ca,* in the buffer with $CaCl_2$; *EDTA,* in the buffer with EDTA. *Columns,* average cell number of three wells; *bars,* SD. *C,* low-shear-force cell adhesion analysis of the other BCP-ALL cell lines. Assay was carried out as above. *White columns,* in the presence of $CaCl_2$; *gray columns,* in the presence of EDTA. *Columns,* average cell number of three wells; *bars,* SD. *D,* Western and selectin blot analyses of NALL-1 cell lysate. *Left,* lysates of NALL-1 cells were subjected to 5.0% SDS-PAGE under reducing conditions and immunoblotted with anti-sLe^X mAb (CSLEX1; *lanes 1* and *2*) and with anti-CD43 mAb (DF-T1; *lanes 3* and *4*). The cell lysates were incubated with or without OSGPEP'ase and subjected to electrophoresis. *Lanes 1* and *3,* without OSGPEP'ase; *lanes 2* and *4,* with OSGPEP'ase. *Right,* NALL-1 cells were left untreated (*lanes 5, 7,* and *9*) or pretreated with OSGPEP'ase during cell culture (*lanes 6, 8,* and *10*). Cell lysates were subjected to 7.5% SDS-PAGE under reducing conditions and analyzed by Western blotting with anti-sLe^X mAb (CSLEX1; *lanes 5* and *6*), selectin blotting with E-selectin/Ig (*E-sel; lanes 7* and *8*), or Western blotting with anti-CD43 mAb (MEM59; *lanes 9* and *10*). *Left,* positions of molecular mass markers; *arrowheads,* positions of the signals.

carrier of E-selectin carbohydrate ligands in NALL-1 cells and that it may be CD43.

BCP-ALL cell lines express not PSGL-1 but CD43. PSGL-1 is known as a major ligand of P-selectin/E-selectin on neutrophils and subsets of T cells. Its molecular mass is similar to that of CD43 under reducing conditions (32), whereas it is ~250 kDa under nonreducing conditions. This is because PSGL-1 forms a disulfide-bonded homodimer. To discriminate CD43 from PSGL-1, we conducted SDS-PAGE under nonreducing conditions using the respective mAbs. PSGL-1 was clearly detected as a ~250-kDa band in HL60 cells but was not detectable in NALL-1 cells, which did not express detectable level of PSGL-1 (Fig. 2*A, top*). These cells were also analyzed with flow cytometry. As shown in Fig. 2*B*, PSGL-1 was not detected in NALL-1 (*top left*), whereas NALL-1 expressed CD43 (*top right*) and control HL60 expressed both PSGL-1 and CD43 (*bottom*). Next, we examined whether PSGL-1 and CD43 were present in the other BCP-ALL cell lines using flow cytometry. Nalm-6, Nalm-16, Nalm-20, KOPN-8, KOPN-K, BV-173, and LAZ221 were negative for PSGL-1 but strongly positive for CD43 (Table 1A, third and fourth columns). These results suggest that the major E-selectin ligand carrier is not PSGL-1 in BCP-ALL cell lines.

Clinical BCP-ALL samples are essentially PSGL-1$^{neg/low}$/CD43^{high}. To investigate whether primary B-precursor ALL cells and BCP-ALL cell lines shared the same characteristic expression of PSGL-1 and CD43, we performed a flow cytometric analysis of BM-derived leukemia cells from the 20 patients with BCP-ALL. For the expression of sialomucins, positivity for CD43 was >85% in 14 of 20 patients and >45% in 20 of 20 patients but PSGL-1 was negative

Table 1. Reactivity with selectin/Ig chimera and expression of sialomucins in BCP-ALL cell lines and BM-derived blast cells from patients with BCP-ALL

	E-selectin/Ig	P-selectin/Ig	PSGL-1	CD43	CD10
A					
Nalm-6	++	−	−	++++	++++
Nalm-16	+	++	−	++++	++++
Nalm-20	++	+++	−	++++	+++
KOPN-8	+++	++	−	+++	+++
KOPN-K	++	+++	−	+++	+++
BV-173	++	+++	−	+++	+++
LAZ221	++	+++	−	++++	+++
HL60	++++	++++	++++	++++	−
Raji	−	−	−	−	−
B					
Patient 1	++	++	±	++++	++++
Patient 2	++	+	−	++++	++++
Patient 3	++	++	+++	++++	−
Patient 4	++	++	+	++++	++++
Patient 5	n.t.	n.t.	±	++++	++++
Patient 6	n.t.	++	n.t.	++++	++++
Patient 7	++	+++	±	++++	+++
Patient 8	+	++++	±	++++	++++
Patient 9	+	+++	±	++++	+++
Patient 10	±	+++	±	++++	++++
Patient 11	+	+++	±	++++	±
Patient 12	n.t.	n.t.	+	++++	−
Patient 13	n.t.	n.t.	±	+++	++
Patient 14	n.t.	n.t.	±	+++	++++
Patient 15	n.t.	n.t.	±	++++	++++
Patient 16	n.t.	n.t.	±	++++	++++
Patient 17	+	+++	±	+++	++++
Patient 18	+	+++	±	++++	++++
Patient 19	n.t.	n.t.	±	+++	++++
Patient 20	+	+++	±	+++	++++

NOTE: A panel of BCP-ALL cell lines, HL60, and Raji cells were investigated for reactivity with selectin/Ig chimera and expression of CD43, PSGL-1, and CD10. BM-derived CD45$^+$ blasts were gated and stained with selectin/Ig chimeras and mAbs for CD43, PSGL-1, and CD10. The reactivity or expression was presented in a semiquantitative manner: ++++, >75% of cells positive; +++, 35% to 75% positive; ++, 15% to 35% positive; +, 5% to 15% positive; ±, 1% to 5% positive; −, <1% of cells positive.
Abbreviation: n.t., not tested.

to very weakly positive in 18 of 19 patients (Table 1B, third and fourth columns); most patients were PSGL-1$^{neg/low}$/CD43^{high}. The cells were PSGL-1^{high}/CD43^{high} (Table 1B) in patient 3. They may have exceptional characteristics whose pathologic meaning is currently unclear. However, these results suggest that the majority of clinical BCP-ALL cells are PSGL-1$^{neg/low}$/CD43^{high}, and BCP-ALL cell lines, including NALL-1, essentially inherit characteristics of primary B-precursor ALL cells.

The major selectin ligand carrier protein gp135 is suggested to be CD43. To test whether gp135 is CD43 or not, we carried out coimmunoprecipitation and selectin pull-down assays. Figure 2C illustrates the results of the coimmunoprecipitation analysis. When the immunoprecipitation was performed with the anti-sLe^X mAb CSLEX1, a band with a molecular mass of ~135 kDa was detected along with additional signals for larger proteins (*lane 1*). The same immunoprecipitated sample clearly contained CD43 with a similar molecular size to gp135 (*lane 2*). In contrast, the immunoprecipitate obtained with anti-CD43 mAb was reactive not only with anti-CD43 but also with CSLEX1 at the same electrophoretic mobility (*lanes 3* and *4*). Figure 2D shows the result of an E-selectin pull-down analysis. The ~135-kDa signal was clearly detected by pull-down with E-selectin (*lane 2*). In contrast, control IgG could not pull-down any significant signal at ~135 kDa (*lane 4*). Although an additional ~220-kDa band was visualized (*lane 2*; *open arrowhead*), the signal was also detected with control IgG (*lane 4*) and thought to be nonspecific. To examine the presence of CD43 in the pull-down fractions, the proteins were released using EDTA from the selectin beads and again immunoprecipitated with anti-CD43 mAb. We could detect the ~135-kDa protein using anti-CD43 mAb (*lane 3*). These results suggest that the major selectin ligand carrier gp135 on NALL-1 cells is CD43.

Effect of CD43 knockdown on cell adhesion activity. The function of CD43 in cell adhesion was investigated in knockdown experiments. The knockdown efficiency of *CD43*-shRNA was 60% in NALL-1siCD43#1 and 49% in NALL-1siCD43#2 cells (Fig. 3A). CD43 expression was examined using flow cytometry and immunoblot analyses (Fig. 3*B* and *C*). The mean fluorescence intensity (MFI) of CD43 in NALL-1siCD43#1 and NALL-1siCD43#2 was 7.6% and 65.2% of the control, respectively (Fig. 3*B*). As shown in Fig. 3*C*, the intensity of CD43 was markedly reduced in NALL-1siCD43#1 cells using the DF-T1 mAb (*lane 3*). CD43 expression in the NALL-1siCD43#2 subline was substantially diminished (*lane 4*). The reactivity with E-selectin/Ig was also evaluated using flow cytometry. Whereas MFI in NALL-1siCD43#2 cells was comparable with that in the parental cells, MFI in the NALL-1siCD43#1 subline decreased to 75% of the control (data not shown).

The effect of knocking down *CD43* was evaluated using functional low-shear-force cell adhesion assays (Fig. 4*A*). For adherence to E-selectin, the knockdown resulted in a 24% decrease in NALL-1siCD43#1 cells (*light gray columns*) and 7% decrease in NALL-1siCD43#2 cells (*striped columns*) compared with control NALL-1scrambled cells (*white columns*). Next, we conducted a rolling assay and the rolling activity of NALL-1 cells was evaluated on CHO-E cells. Under a constant shear stress of 5 dyne/cm^2, we detected significant NALL-1 cell rolling on CHO-E cells in the buffer containing $CaCl_2$ (Fig. 4*B* and *C*). Rolling events in NALL-1siCD43#1 and NALL-1siCD43#2 cells were significantly reduced (69% for #1 versus control, $P < 0.001$; 35% for #2 versus control, $P < 0.001$; Fig. 4*B*). For rolling velocity, knockdown of *CD43* resulted in a significant increase compared with the control (168% for #1 versus control, $P < 0.001$; 135% for #2 versus control, $P < 0.005$; Fig. 4*C*). These results suggest that CD43 on NALL-1 cells functions as an E-selectin ligand.

Down-regulation of CD43 inhibits tissue engraftment. Finally, we examined the effect of knocking down *CD43* on tissue migration using a mouse model. We chose NALL-1siCD43#1 cells for the cell migration assay *in vivo* using NOD/SCID mice. In the assay, parental NALL-1 cells essentially behaved like the NALL-1scrambled cells (Fig. 4*D*, *white columns*). We observed that more cells migrated to BM than those to spleen and liver at 6 h. Few cells were detected in peripheral blood. Migrated cells were also found at 24 h and their number was similar to that at 6 h. This observation suggested that the leukemic cells engraft to the peripheral lymphoid organs, not a simple transient migration. As shown in Fig. 4*D*, the migration/engraftment of the knockdown cells (*black columns*) decreased significantly compared with that of the scrambled cells (5–20%; *white columns*). The decrease at 24 h was similar to that at 6 h. To exclude any possible reduction in levels of other cell adhesion molecules by the knockdown, we examined the expression of

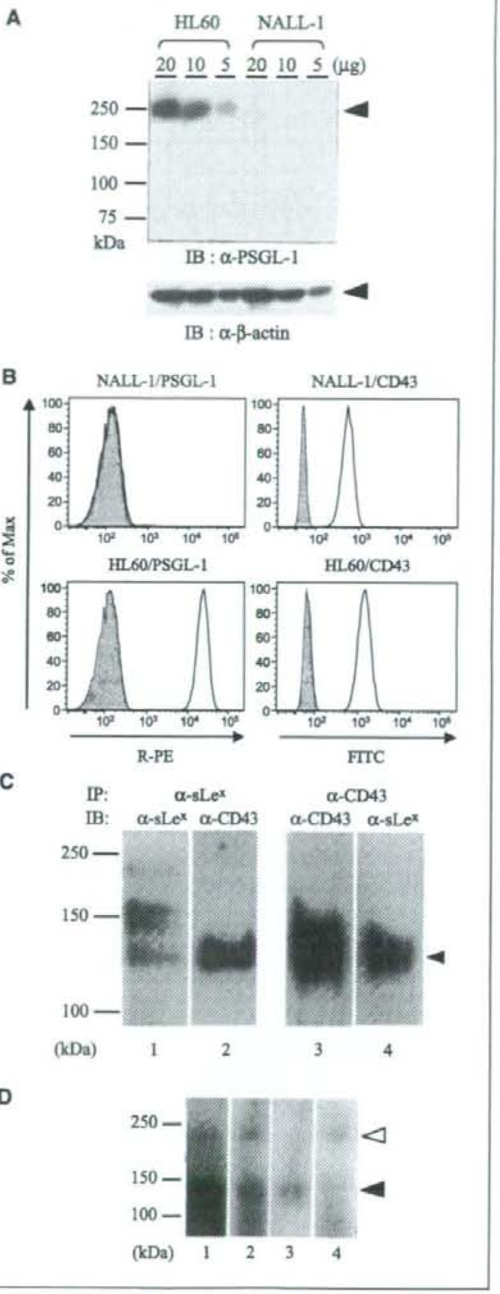

Figure 2. Expression of the E-selectin counter-receptor candidate in NALL-1 cells. *A*, lysates from NALL-1 and HL60 cells were subjected to SDS-PAGE under nonreducing conditions and immunoblotted with anti-PSGL-1 (KPL-1; *top*) or anti-β-actin (AC-15; *bottom*) antibody. *Left*, positions of molecular mass markers; *arrowheads*, positions of the signals. *B*, NALL-1 and HL60 cells were stained with anti-PSGL-1 and CD43 mAbs (KPL-1 and 1G10, respectively), and cell surface expression of sialomucin was detected using flow cytometry. *C*, coimmunoprecipitation of sLe^X carbohydrate antigen with CD43. NALL-1 cell lysates were immunoprecipitated (*IP*) with anti-sLe^X (CSLEX1; *lanes 1* and *2*) or anti-CD43 mAb (MEM59; *lanes 3* and *4*). Precipitates were subjected to SDS-PAGE under reducing conditions and immunoblotted (*IB*) with anti-sLe^X (CSLEX1; *lanes 1* and *4*) or anti-CD43 mAb (MEM59; *lanes 2* and *3*). *D*, selectin pull-down from cell lysates. NALL-1 cell surface proteins were biotinylated, subjected to SDS-PAGE under reducing conditions, and blotted with streptavidin-HRP and a chemiluminescence substrate. *Lane 1*, total lysate; *lane 2*, precipitates of the pull-down by E-selectin/Ig; *lane 4*, precipitates of the pull-down by control human IgG. *Lane 3*, to further show the pull-down of CD43 by selectins, precipitates obtained with E-selectin/Ig were released using EDTA and again precipitated with anti-CD43 mAb (MEM59). *C* and *D*, *closed arrowheads*, positions of the major carrier glycoprotein (gp135) and CD43; *left*, positions of molecular mass markers. *D*, *open arrowhead*, position of the nonspecific pull-down protein. *A* to *D*, data are representative of multiple independent experiments.

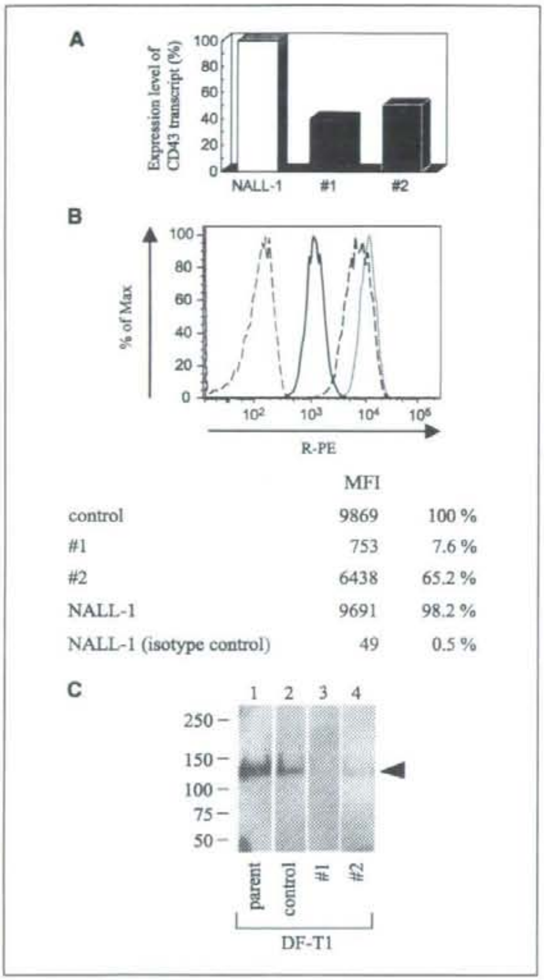

	MFI	
control	9869	100 %
#1	753	7.6 %
#2	6438	65.2 %
NALL-1	9691	98.2 %
NALL-1 (isotype control)	49	0.5 %

Figure 3. Suppression of CD43 expression on NALL-1 cells by shRNA for *CD43*. *A*, expression of *CD43* transcript in shRNA-introduced NALL-1 cells. The relative expression of *CD43* was calculated as the percentage of the value obtained for the parental NALL-1, which was set as 100. *B*, *top*, CD43 expression in NALL-1 cell sublines transfected with shRNA for *CD43*. The surface expression of CD43 was analyzed using DF-T1. *Dotted line*, control NALL-1 cells (scrambled shRNA-introduced NALL-1); *solid line*, NALL-1siCD43#1; *dark dashed line*, NALL-1siCD43#2; *gray dashed line*, isotype-matched control. *Bottom*, the relative expression of CD43 was also presented as MFI and percentage (%) compared with the positive control NALL-1scrambled cells. *C*, immunoblot analysis of NALL-1 cells transfected with shRNA. Lysates of shRNA-transfected NALL-1 cells were analyzed by Western blotting with anti-CD43 mAb DF-T1. *parent*, parental NALL-1 cells; *control*, NALL-1scrambled; *#1*, NALL-1siCD43#1; *#2*, NALL-1siCD43#2. *Left*, positions of molecular mass markers; *arrowhead*, position of CD43.

several cell adhesion molecules and gelatinase activity (Table 2). The levels of integrin β_1, VLA4α, integrin β_2, LFA1α, ICAM-1, L-selectin, CD44, CCR7, CXCR5, CCR6, CXCR3, CXCR4, *MMP2*, and *MMP9* and gelatinase activity did not decrease significantly in NALL-1siCD43#1 cells compared with NALL-1control cells. These results suggest that the down-regulation of CD43 results in an inhibition of cell migration from the vascular system to peripheral tissues and that CD43 plays a significant role in mediating the extravasation of NALL-1 cells.

Discussion

Thus far, PSGL-1, ESL-1, L-selectin, and CD44 have been reported as selectin counter-receptors. In BCP leukemia cells, the major selectin ligand carrier was first shown as a 150-kDa *O*-glycosylated protein (17, 18). L-selectin (33, 34) and CD44 (35, 36) are ruled out because of their molecular sizes, ~70 and ~85 kDa, respectively. ESL-1 is 150 kDa but an *N*-glycosylated protein (37). As demonstrated in the present study, PSGL-1 is essentially negative and the most feasible candidate of the major selectin ligand carrier on BCP-ALL cells is a sialomucin, CD43. In a study of T-cell recruitment to skin, the cutaneous lymphocyte-associated antigen (CLA) was reported as the only E-selectin/P-selectin ligand and located on PSGL-1 (38, 39). Recently, however, CD43 was reported as a ligand for E-selectin on CLA$^+$ T cells (32). CD43 was also found to be an E-selectin ligand in activated T cells (40). It is worth noting that PSGL-1 as well as CD43 are present under physiologic conditions in both human CLA$^+$ T cells and mouse Th1 cells (22, 32, 38–41). CD43 must function in cooperation with PSGL-1 and the central player may be PSGL-1 *in vivo*.

There are two major glycoforms of CD43 (135/115 kDa) in human T cells (42). The 115-kDa form is found on resting T, whereas the 135-kDa CD43 is expressed on activated T cells. Core 2–branched *O*-glycans are abundant in the larger glycoform and biosynthesis of the branch is regulated by the rate-limiting C2GnT1 (43). Its expression is up-regulated during T-cell and B-cell activation (42, 44). According to our previous investigations, C2GnT1 and carbohydrate selectin ligand are highly expressed in BCP-ALL cells and down-regulated simultaneously to 1 of 10 during differentiation, and the expression level of carbohydrate selectin ligand is regulated by C2GnT1 (12, 17–19). Applying our previous findings to the present results, C2GnT1 is thought to regulate the biosynthesis of core 2 branches on CD43 in BCP-ALL cells. The changes of CD43 glycoforms during pre-B-cell differentiation will be reported elsewhere.[8]

Our immunophenotypic observations and functional data on CD43 obtained using NALL-1 cells may be applicable to most B-precursor ALL patients. Of course, we do not exclude the possibility that the major carrier of carbohydrate selectin ligand is not CD43 or PSGL-1 but another *O*-glycoprotein on primary BCP-ALL cells. For selectin-related adhesion molecules, there are sulfated carbohydrate structures, including 6′-sulfo-sLe^X, 6-sulfo-sLe^X, 6,6′-disulfo-sLe^X, and sulfo-Le^X (45). Some of such structures have been proved as L-selectin ligands and may be possibly expressed in BCP-ALL cells and involved in the leukemic cell migration to peripheral tissues. However, it requires careful and extensive investigation to draw definitive conclusion. According to our recent data, it is suggested that primary precursor B cells express genuine sLe^X epitopes[9] and it may be involved in the trafficking of pre-B cells to BM.

---

[8] H. Sasaki, J. Kikuchi, H. Ohno, C. Nonomura, Y. Furukawa, and M. Nakamura, unpublished data.

[9] J. Kikuchi, H. Sasaki, C. Nonomura, H. Ohno, Y. Furukawa, and M. Nakamura, unpublished data.

Selectin-binding activity measured by flow cytometry may not necessarily reflect the actual function of a carbohydrate ligand and its carrier protein. That is, we detected P-selectin binding using flow cytometry but could not observe a significant adhesion capability of NALL-1 cells to P-selectin–immobilized surfaces in low-shear-stress cell adhesion assay (Fig. 1*B* and *C*). Likewise, we observed some discrepancies about the effects of knocking down the expression of CD43 and functional assays. Whereas NALL-1siCD43#1 and NALL-1siCD43#2 cells showed 60% and 49% decrease in the expression of CD43 transcript, the immunoreactivity for anti-CD43 mAb using flow cytometry exhibited 92% and 35% suppression, respectively (Fig. 3*A* and *B*). The knocking down of CD43 resulted in only 25% and 7% decrease in #1 and #2 cells on low-shear-force cell adhesion assay, respectively (Fig. 4*A*). The reactivity profile of the mAb in the flow cytometry assay may be very sensitive as for NALL-1siCD43#1 cells. Similarly, the reactivity profile of low-shear-force cell adhesion assay may be also sensitive for both #1 and #2 cells and rolling substrate E-selectin. Besides these, the knocking down effect of CD43 in NALL-1siCD43#1 (60%; Fig. 3*A*) was well correlated to the decrease in cell rolling events (69%; Fig. 4*B*), increase in cell rolling velocity (168%; Fig. 4*C*), and suppressed cell migration *in vivo* (70–75%; Fig. 4*D*).

For PSGL-1, a versatile mAb KPL-1 has been developed (46). It blocks adhesion of PSGL-1 with P-selectin. The development of a novel tool, such as a functional mAb, to block the interaction of CD43 with E-selectin is required to make further analyses

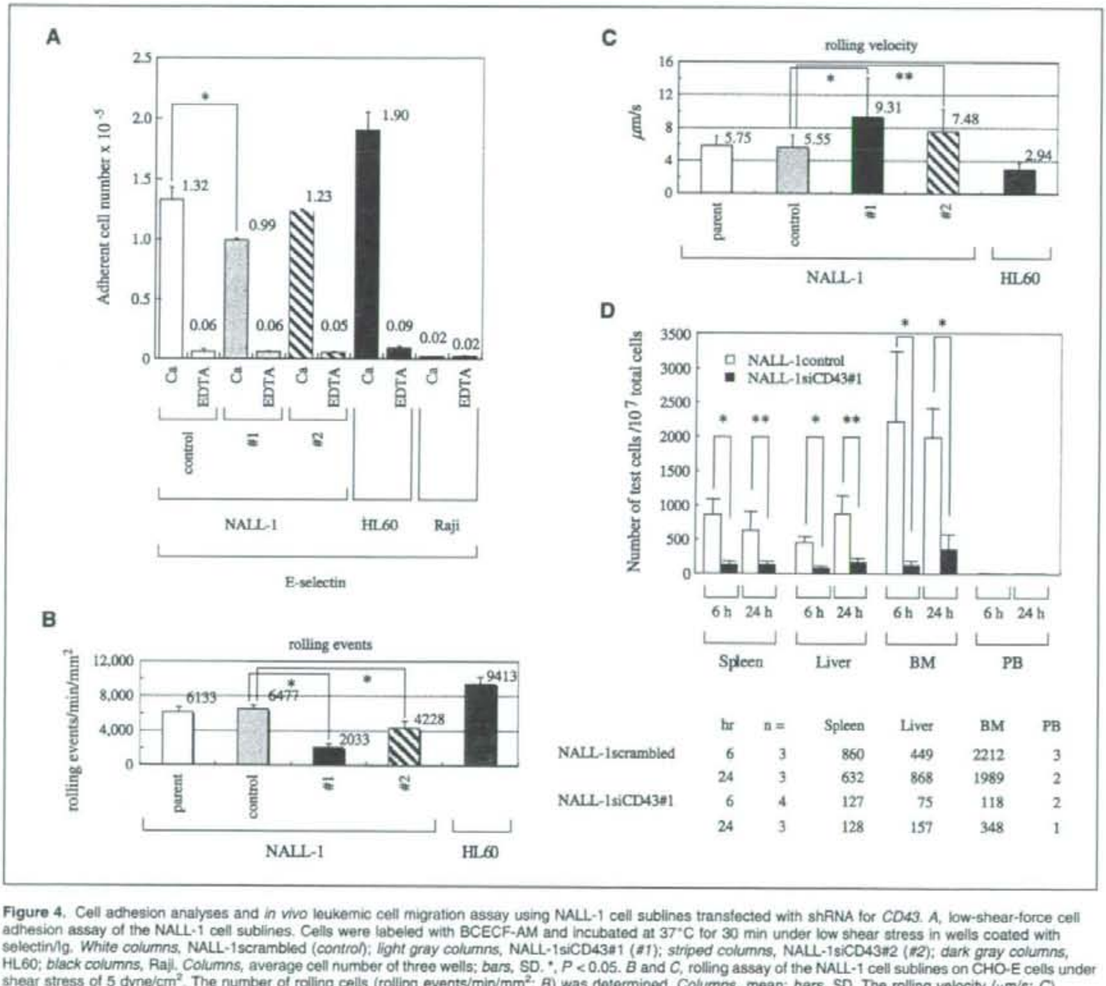

	hr	n =	Spleen	Liver	BM	PB
NALL-1scrambled	6	3	860	449	2212	3
	24	3	632	868	1989	2
NALL-1siCD43#1	6	4	127	75	118	2
	24	3	128	157	348	1

Figure 4. Cell adhesion analyses and *in vivo* leukemic cell migration assay using NALL-1 cell sublines transfected with shRNA for *CD43*. *A*, low-shear-force cell adhesion assay of the NALL-1 cell sublines. Cells were labeled with BCECF-AM and incubated at 37°C for 30 min under low shear stress in wells coated with selectin/Ig. *White columns*, NALL-1scrambled (*control*); *light gray columns*, NALL-1siCD43#1 (*#1*); *striped columns*, NALL-1siCD43#2 (*#2*); *dark gray columns*, HL60; *black columns*, Raji. *Columns*, average cell number of three wells; *bars*, SD. *, $P < 0.05$. *B* and *C*, rolling assay of the NALL-1 cell sublines on CHO-E cells under shear stress of 5 dyne/cm^2. The number of rolling cells (rolling events/min/mm^2; *B*) was determined. *Columns*, mean; *bars*, SD. The rolling velocity (μm/s; *C*) was calculated. *Columns*, average of 25 cells traced; *bars*, SD. *White columns*, parental NALL-1; *light gray columns*, NALL-1scrambled; *black columns*, NALL-1siCD43#1; *striped columns*, NALL-1siCD43#2; *dark gray columns*, HL60. *, $P < 0.001$; **, $P < 0.005$. *D*, *in vivo* leukemic cell migration assay using immunodeficient mice. TRITC-labeled test cells and CFSE-labeled control cells (1:1) were injected to NOD/SCID mice. The cell number in peripheral blood (*PB*) and engrafted cell number in the cell suspension from spleen, liver, and BM were counted using flow cytometry. *Columns*, average cell number of the recovered test cells of independent experiments; *bars*, SD. *White columns*, NALL-1scrambled; *black columns*, NALL-1siCD43#1. *, $P < 0.01$; **, $P < 0.05$.

Table 2. Expression of cell adhesion molecules and gelatinase activity in the BCP-ALL cell line NALL-1 and its sublines

	NALL-1	NALL-1scrambled (NALL-1control)	NALL-1siCD43#1	Positive control cells*
A				
Integrin β$_1$	±	±	±	++++*
VLA4α	++++	++++	++++	n.t.
Integrin β$_2$	+++	++	+++	n.t.
LFA1α	++	++	++	n.t.
ICAM-1	+++	+++	+++	n.t.
L-selectin	++++	++++	++++	n.t.
CD44	++++	++++	++++	n.t.
CCR7	++	+	+	n.t.
CXCR5	±	±	±	+++*
CCR6	±	±	±	+++*
CXCR3	++	+	+	n.t.
CXCR4	+++	++	+++	n.t.
B				
MMP2	15 ± 8	18 ± 5	17 ± 7	100 ± 17
MMP9	7 ± 3	6 ± 2	7 ± 2	100 ± 12
C				
Gelatinase activity	10 ± 4	10 ± 3	9 ± 4	100 ± 26

NOTE: (A) Flow cytometric expression of cell adhesion molecules was examined using specific mAbs in the parental NALL-1, NALL-1siCD43#1, and NALL-1scrambled cells. The expression was presented in a semiquantitative manner: ++++, >75% of cells positive; +++, 35% to 75% positive; ++, 15% to 35% positive; +, 5% to 15% positive; ±, 1% to 5% positive; −, <1% of cells positive. (B) *MMP2* and *MMP9* expression was examined using real-time PCR in the parental NALL-1, NALL-1siCD43#1, and NALL-1scrambled cells. The relative expression is calculated as the percentage of the value obtained for the control HL60, which is set as 100, and presented as mean ± SD. (C) Gelatinase activity was measured using gelatin zymography in CXCL12-treated parental NALL-1, NALL-1siCD43#1, and NALL-1scrambled cells. The relative activity is calculated as the percentage of the value obtained for the control HL60, which is set as 100, and presented as mean ± SD.

*Positive control cells are HL60 for integrin β$_1$, Raji for CXCR5 and CCR6, and HL60 for *MMP2*, *MMP9*, and gelatinase activity, respectively.

possible. Recently, an anti-CD44 mAb is reported to have the ability to purge leukemic stem cells from niches (6, 7). The data presented here indicate that a functional anti-CD43 mAb could also be of potential use in purging BCP-ALL cells from microenvironmental niches.

Acknowledgments

Received 4/19/2007; revised 12/1/2007; accepted 12/4/2007.

Grant support: Core Research for Evolution Science and Technology of Japan Science and Technology Agency, Japan Leukemia Research Fund (M. Nakamura), and Glycoengineering Project (Technological Development to Facilitate the Use of Sugar Chain Functions) of New Energy and Industrial Technology Development Organization.

The costs of publication of this article were defrayed in part by the payment of page charges. This article must therefore be hereby marked *advertisement* in accordance with 18 U.S.C. Section 1734 solely to indicate this fact.

We thank Dr. Luk Van Parijs for kindly providing pLL3.7; Drs. Isao Miyoshi and Ichiro Kubonishi (Kochi Medical School, Nankoku, Japan) for generously supplying NALL-1; Drs. Yoshinobu Matsuo and Akira Harashima (Fujisaki Cell Center, Hayashibara Research Institute, Okayama, Japan) for the BCP-ALL cell lines; Hironobu Sasaki, Hiroyuki Ohno, Yumi Nakamichi, Nana Matsuura, Kazunori Nakamura, and Hirotaka Shinohara for their technical assistance; and Etsuko Hiraide for her secretarial assistance.

References

1. Henderson ES, Lister TA, Greaves MF. Leukemia. 7th ed. Philadelphia (PA): W.B. Saunders; 2002.
2. Wiernik PH, Goldman JM, Dutcher JP, Kyle RA. Neoplastic disease of the blood. 4th ed. Cambridge (UK): Cambridge University Press; 2003.
3. Wang JC, Dick JE. Cancer stem cells: lessons from leukemia. Trends Cell Biol 2005;15:494–501.
4. Matsunaga T, Takemoto N, Sato T, et al. Interaction between leukemic-cell VLA-4 and stromal fibronectin is a decisive factor for minimal residual disease of acute myelogenous leukemia. Nat Med 2003;9:1158–65.
5. Lapidot T, Dar A, Kollet O. How do stem cells find their way home? Blood 2005;106:1901–10.
6. Krause DS, Lazarides K, von-Andrian UH, Van-Etten RA. Requirement for CD44 in homing and engraftment of BCR-ABL-expressing leukemic stem cells. Nat Med 2006;12:1175–80.
7. Jin L, Hope KJ, Zhai Q, Smadja-Joffe F, Dick JE. Targeting of CD44 eradicates human acute myeloid leukemic stem cells. Nat Med 2006;12:1167–74.
8. Copelan EA, McGuire EA. The biology and treatment of acute lymphoblastic leukemia in adults. Blood 1995;85:1151–68.
9. Middleton J, Patterson AM, Gardner L, Schmutz C, Ashton BA. Leukocyte extravasation: chemokine transport and presentation by the endothelium. Blood 2002;100:3853–60.
10. Kannagi R. Regulatory roles of carbohydrate ligands for selectins in the homing of lymphocytes. Curr Opin Struct Biol 2002;12:599–608.
11. Kansas GS. Selectins and their ligands: current concepts and controversies. Blood 1996;88:3259–87.
12. Kikuchi J, Ozaki H, Nonomura C, et al. Transfection of antisense core 2 β1,6-*N*-acetylglucosaminyltransferase-1 cDNA suppresses selectin ligand expression and tissue infiltration of B-cell precursor leukemia cells. Leukemia 2005;19:1934–40.
13. Bradstock KF, Makrynikola V, Bianchi A, Shen W, Hewson J, Gottlieb DJ. Effects of the chemokine stromal cell-derived factor-1 on the migration and localization of precursor-B acute lymphoblastic leukemia cells within bone marrow stromal layers. Leukemia 2000;14:882–8.
14. Tokoyoda K, Egawa T, Sugiyama T, Choi BI, Nagasawa T. Cellular niches controlling B lymphocyte behavior within bone marrow during development. Immunity 2004;20:707–18.
15. Hara J, Matsuda Y, Fujisaki H, et al. Expression of adhesion molecules in childhood B-lineage-cell neoplasms. Int J Hematol 2000;72:69–73.
16. Ashley DM, Bol SJ, Tucker DP, Waugh CM, Kannourakis G. Flow cytometric analysis of intercellular adhesion between B-cell precursor acute lymphoblastic leukemic cells and bone marrow stromal cells. Leukemia 1995;9:58–67.
17. Nakamura M, Furukawa Y, Sasaki R, et al. UDP-GlcNAc:Galβ1→3GalNAc (GlcNAc to GalNAc) β1→6*N*-acetylglucosaminyltransferase holds a key role on the

control of CD15s expression in human pre-B lymphoid cell lines. Glycobiology 1999;9:1–12.

18. Nakamura M, Kudo T, Narimatsu H, et al. Single glycosyltransferase, core 2 β1,6-*N*-acetylglucosaminyltransferase, regulates cell surface sialyl-Le^{X} expression level in human pre-B lymphocytic leukemia cell line KM3 treated with phorbolester. J Biol Chem 1998;273:26779–89.

19. Kikuchi J, Shinohara H, Nonomura C, et al. Not core 2 β1,6-*N*-acetylglucosaminyltransferase-2 and -3 but -1 regulates sialyl-Lewis-X expression in human precursor-B cell. Glycobiology 2005;15:271–80.

20. McEver RP, Cummings RD. Role of PSGL-1 binding to selectins in leukocyte recruitment. J Clin Invest 1997;100:S97–103.

21. Xia L, Sperandio M, Yago T, et al. P-selectin glycoprotein ligand-1-deficient mice have impaired leukocyte tethering to E-selectin under flow. J Clin Invest 2002;109:939–50.

22. Hirata T, Merrill-Skoloff G, Aab M, Yang J, Furie BC, Furie B. P-selectin glycoprotein ligand 1 (PSGL-1) is a physiological ligand for E-selectin in mediating T helper 1 lymphocyte migration. J Exp Med 2000;192:1669–76.

23. Yago T, Tsukuda M, Tajima H, et al. Analysis of initial attachment of B cells to endothelial cells under flow conditions. J Immunol 1997;158:707–14.

24. Rubinson DA, Dillon CP, Kwiatkowski AV, et al. A lentivirus-based system to functionally silence genes in primary mammalian cells, stem cells and transgenic mice by RNA interference. Nat Genet 2003;33:401–6.

25. Lawrence MB, McIntire LV, Eskin SG. Effect of flow on polymorphonuclear leukocyte/endothelial cell adhesion. Blood 1987;70:1284–90.

26. Kanamori A, Kojima N, Uchimura K, et al. Distinct sulfation requirements of selectins disclosed using cells that support rolling mediated by all three selectins under shear flow. J Biol Chem 2002;277:32578–86.

27. Scimone ML, Aifantis I, Apostolou I, Boehmer Hv, Andrian UHv. A multistep adhesion cascade for lymphoid progenitor cell homing to the thymus. Proc Natl Acad Sci U S A 2006;103:7006–11.

28. Nijmeijer BA, Mollevanger P, van-Zelderen-Bhola SL, Kluin-Nelemans HC, Willemze R, Falkenburg JH. Monitoring of engraftment and progression of acute lymphoblastic leukemia in individual NOD/SCID mice. Exp Hematol 2001;29:322–9.

29. Garcia-Vicuña R, Gómez-Gaviro MV, Dominguez-Luis MJ, et al. CC and CXC chemokine receptors mediate migration, proliferation, and matrix metalloproteinase production by fibroblast-like synoviocytes from rheumatoid arthritis patients. Arthritis Rheum 2004;50:3866–77.

30. Hiraki S, Miyoshi I, Kubonishi I, et al. Human leukemic "null" cell line (NALL-1). Cancer 1977;40:2131–5.

31. Matsuo Y, Drexler HG. Establishment and characterization of human B cell precursor-leukemia cell lines. Leuk Res 1998;22:567–79.

32. Fuhlbrigge RC, King SL, Sackstein R, Kupper TS. CD43 is a ligand for E-selectin on CLA^{+} human T cells. Blood 2006;107:1421–6.

33. Picker LJ, Warnock RA, Burns AR, Doerschuk CM, Berg EL, Butcher EC. The neutrophil selectin LECAM-1 presents carbohydrate ligands to the vascular selectins ELAM-1 and GMP-140. Cell 1991;66:921–33.

34. Zöllner O, Lenter MC, Blanks JE, et al. L-selectin from human, but not from mouse neutrophils binds directly to E-selectin. J Cell Biol 1997;136:707–16.

35. Dimitroff CJ, Lee JY, Rafii S, Fuhlbrigge RC, Sackstein R. CD44 is a major E-selectin ligand on human hematopoietic progenitor cells. J Cell Biol 2001;153:1277–86.

36. Katayama Y, Hidalgo A, Chang J, Peired A, Frenette PS. CD44 is a physiological E-selectin ligand on neutrophils. J Exp Med 2005;201:1183–9.

37. Steegmaier M, Levinovitz A, Isenmann S, et al. The E-selectin-ligand ESL-1 is a variant of a receptor for fibroblast growth factor. Nature 1995;373:615–20.

38. Fuhlbrigge RC, Kieffer JD, Armerding D, Kupper TS. Cutaneous lymphocyte antigen is a specialized form of PSGL-1 expressed on skin-homing T cells. Nature 1997;389:978–81.

39. Fuhlbrigge RC, King SL, Dimitroff CJ, Kupper TS, Sackstein R. Direct real-time observation of E- and P-selectin-mediated rolling on cutaneous lymphocyte-associated antigen immobilized on Western blots. J Immunol 2002;168:5645–51.

40. Matsumoto M, Atarashi K, Umemoto E, et al. CD43 functions as a ligand for E-selectin on activated T cells. J Immunol 2005;175:8042–50.

41. Austrup F, Vestweber D, Borges E, et al. P- and E-selectin mediate recruitment of T-helper-1 but not T-helper-2 cells into inflammed tissues. Nature 1997;385:81–3.

42. Fukuda M, Tsuboi S. Mucin-type *O*-glycans and leukosialin. Biochim Biophys Acta 1999;1455:205–17.

43. Bierhuizen MF, Maemura K, Fukuda M. Expression of a differentiation antigen and poly-*N*-acetyllactosaminyl *O*-glycans directed by a cloned core 2 β-1,6-*N*-acetylglucosaminyltransferase. J Biol Chem 1994;269:4473–9.

44. Nakamura M, Ishida T, Kikuchi J, Furukawa Y, Matsuda M. Simultaneous core 2 β1→6*N*-acetylglucosaminyltransferase up-regulation and sialyl-Le^{X} expression during activation of human tonsillar B lymphocytes. FEBS Lett 1999;463:125–8.

45. Mitsuoka C, Sawada-Kasugai M, Ando-Furui K, et al. Identification of a major carbohydrate capping group of the L-selectin ligand on high endothelial venules in human lymph nodes as 6-sulfo sialyl Lewis X. J Biol Chem 1998;273:11225–33.

46. Snapp KR, Ding H, Atkins K, Warnke R, Luscinskas FW, Kansas GS. A novel P-selectin glycoprotein ligand-1 monoclonal antibody recognizes an epitope within the tyrosine sulfate motif of human PSGL-1 and blocks recognition of both P- and L-selectin. Blood 1998;91:154–64.

Annals of Oncology 20: 166–174, 2009
doi:10.1093/annonc/mdn562

Childhood cancer in Japan: focusing on trend in mortality from 1970 to 2006

L. Yang[1], J. Fujimoto[2], D. Qiu[1] & N. Sakamoto[1]*

[1]Department of Maternal and Child Health, National Research Institute for Health and Development; [2]National Research Institute for Health and Development, Tokyo, Japan

Received 11 July 2008; accepted 14 July 2008

Objective: This paper describes the mortality rates and trends from childhood cancer at the population level over a 37-year period in Japan and other developed countries.

Materials and methods: Age-standardized mortality rates were calculated by the direct method using age-specific mortality rates at 5-year age intervals and weights based on the age distribution of the standard world population. The joinpoint regression model was used to describe changes in trends.

Results: For all cancers combined, the mortality rate during 2000–2006 was 2.20 per 100 000 population for boys and 1.89 for girls. Mortality for all cancers combined decreased since 1970s in Japan. A stable trend was observed in recent 5 years for girls. For leukemia, a declining trend was observed in the whole period for girls and in 1978–2006 for boys. Mortality rates for childhood central nervous system tumors have remained stable at a low level during 1980–2006.

Conclusions: The present study provides updated figures and trends in childhood cancer mortality in Japan and other developed countries. This will help to estimate care needs and to plan intervention and the quantity of appropriate childhood cancer treatment.

Key words: cancer, childhood, epidemiology, mortality, time trends

introduction

It is estimated that ~3000 Japanese children aged from birth to 18 years will develop cancer. Although childhood cancer is rare compared with adult cancer, it is the fourth most common cause of death among children aged 0–14 years in Japan, according to the report given by the Ministry of Health, Labor and Welfare of Japan in 2005. A population-based study in Osaka prefecture in Japan indicated that death due to childhood cancer declined from 1972 to 1995, while the incidence increased in the same period [1]. In the United States, an estimated 10 400 new cases and 1545 deaths are expected to occur among children aged 0–14 years in 2007 [2]. During recent three decades, the incidence of childhood cancer increased ~0.6% annually. In contrast, mortality from childhood cancer declined by 1.3% per year during 1990–2004 [3]. A population-based study among European children since the 1970s showed that the overall incidence of childhood cancer has increased by 1.0% per year, while mortality has declined by 3.6% per year in the past three decades [4, 5].

The decrease in mortality from childhood cancer has been suggested to be due to the effects of improvements in diagnosis and therapy. For all childhood cancers combined, 5-year relative survival has improved markedly over the past three decades, from <50% before the 1970s to ~80% today [2].

There is no national childhood cancer registry system in Japan, and recent childhood cancer mortality has not been well characterized in terms of temporal and geographic trends. This paper describes the occurrence of death from childhood cancer at the population level over a 37-year period in Japan using official death certification data, which record 100% of deaths in Japan. The aim of this study was to ascertain the general mortality trend for each sex and to study the moment at which a shift in the trend occurred.

materials and methods

The number of death by cause, stratified for sex and by 5-year age group for cancer for the period 1970–2006, was derived from vital statistics compiled by the Ministry of Health, Labor and Welfare of Japan. Population figures were obtained from census data and intercensus estimates, by calendar year, age and gender. Population censuses of Japan are conducted every 5 years by the Statistics Bureau, Ministry of Internal Affair and Communications. For comparison, we also calculated the cancer mortality rate in other developed countries, including Canada (1970–2004), the United States (1970–2005), Italy (1970–2003), UK (1970–2005) and New Zealand (1970–2004). Deaths at age 0–4, 5–9 and 10–14 years were derived from the World Health Organization (WHO)

---

*Correspondence to: Dr N. Sakamoto, The Division of Epidemiology, Department of Maternal and Child Health, National Research Institute for Child Health and Development, 2-10-1 Ookura, Setagaya-ku, Tokyo 157-8535, Japan. Tel: +81-03-3416-0181(4360); Fax: +81-03-5494-7490; E-mail: sakamoto@nch.go.jp

mortality database. Estimates of the population, generally based on official censuses, were based on the same WHO database.

During the study period, three different revisions of the International Classification of Disease were used. In Japan, this included International Classification of Diseases (ICD)-8 from 1970 to 1978, ICD-9 from 1979 to 1994 and ICD-10 from 1995 onward. Since the differences were minor in various revisions, we recorded six cancer sites, including all cancer combined (ICD-8: 140–209; ICD-9: 140–208; ICD-10: C00–97), leukemia (ICD-8: 204–207; ICD-9: 204–208; ICD10: C91–C95), lymphomas (ICD-8: 200–202; ICD-9: 200–202; ICD-10: C81–85), central nervous system (CNS) tumors (ICD-9: 191–192; ICD-10: C70–C72), malignant kidney tumors (ICD-8: 189; ICD-9: 189; ICD-10: C64–C68) and malignant bone tumors (ICD-9: 170; ICD-10: C40–C41). In order to avoid possible bias due to changed ICD, the analysis of CNS tumors, malignant bone tumors and lymphomas (United States only) was restricted to data from 1980 onwards.

Age-standardized mortality rates were calculated by the direct method using age-specific mortality rates for 5-year age intervals and weights based on the age distribution of the standard world population. All rates are expressed per 100 000 children-years.

Table 1. Childhood cancer mortality rate (per 100 000) in Japan and other selected countries (boys)

Period of death	Japan	Canada	United States	Italy	UK	New Zealand
Total malignant tumors						
1970–1974	6.19	7.69	6.47	8.72	7.20	8.45
1975–1979	5.86	6.10	5.25	7.96	6.53	7.59
1980–1984	4.99	5.34	4.60	6.96	5.06	7.04
1985–1989	4.13	4.52	3.74	5.50	4.13	7.17
1990–1994	3.37	3.43	3.33	5.40	3.96	4.94
1995–1999	2.90	2.82	2.87	4.53	3.42	4.83
2000–	2.20	2.65	2.68	3.64	3.00	3.58
Leukemia						
1970–1974	3.39	3.58	2.90	3.94	3.02	3.44
1975–1979	3.10	2.81	2.23	3.50	2.79	3.07
1980–1984	2.46	2.06	1.76	2.85	2.11	2.89
1985–1989	1.91	1.79	1.41	2.20	1.52	2.76
1990–1994	1.54	1.17	1.20	1.99	1.41	1.69
1995–1999	1.21	0.90	0.97	1.64	1.18	1.99
2000–	0.84	0.85	0.85	1.25	0.91	0.78
Lymphomas						
1970–1974	0.61	0.76	–	1.14	0.73	0.77
1975–1979	0.66	0.62	–	0.86	0.65	0.75
1980–1984	0.65	0.49	0.39	0.62	0.40	0.51
1985–1989	0.55	0.32	0.31	0.51	0.29	0.58
1990–1994	0.36	0.21	0.23	0.47	0.25	0.15
1995–1999	0.18	0.16	0.16	0.41	0.20	0.23
2000–	0.14	0.12	0.12	0.27	0.20	0.12
Central nervous system tumors						
1980–1984	0.40	1.17	0.95	1.41	1.12	1.50
1985–1989	0.40	1.18	0.86	1.05	1.10	1.66
1990–1994	0.46	0.97	0.86	1.19	1.10	1.79
1995–1999	0.49	0.83	0.79	0.93	0.94	1.35
2000–	0.43	0.81	0.75	0.87	0.85	1.43
Malignant kidney tumors						
1970–1974	0.18	0.35	0.24	0.45	0.33	0.34
1975–1979	0.16	0.20	0.17	0.34	0.26	0.33
1980–1984	0.12	0.13	0.14	0.23	0.20	0.24
1985–1989	0.09	0.10	0.10	0.19	0.09	0.22
1990–1994	0.07	0.06	0.09	0.13	0.12	0.26
1995–1999	0.06	0.05	0.08	0.13	0.13	0.09
2000–	0.05	0.12	0.08	0.09	0.09	0.08
Malignant bone tumors						
1980–1984	0.15	0.18	0.16	0.33	0.26	0.12
1985–1989	0.15	0.16	0.12	0.24	0.18	0.30
1990–1994	0.14	0.11	0.11	0.19	0.14	0.04
1995–1999	0.13	0.12	0.11	0.14	0.13	0.17
2000–	0.09	0.12	0.13	0.15	0.15	0.24

The joinpoint regression model was used to describe changes in trends [6]. We allowed for up to four joinpoints for each model. The computation of mortality rates and their standard errors was implemented in SAS 9.0. Joinpoint analyses were carried out using Joinpoint software 3.3.1 from the Surveillance Research Program of the US National Cancer Institute. Time trends were assessed for all childhood cancer combined and for six major categories, including leukemia, lymphoma, malignant brain tumor, malignant kidney tumor and malignant bone tumor.

The standardized mortality ratio (SMR) by sex was calculated for 47 prefectures in Japan by taking the ratio of the observed to expected deaths. The z-value was computed for each SMR, on the basis of the assumption that observed deaths follow a Poisson distribution. The maps were developed using adjusted SMR by gender.

results

mortality

Tables 1 and 2 give age-adjusted mortality rates in Japan and five other developed countries for all malignant tumors and for

Table 2. Childhood cancer mortality rate (per 100 000) in Japan and other selected countries (girls)

Period of death	Japan	Canada	United States	Italy	UK	New Zealand
Total malignant tumors						
1970–1974	5.10	6.12	5.13	6.90	5.55	6.85
1975–1979	4.61	4.83	4.07	5.90	4.69	6.35
1980–1984	3.88	4.24	3.59	5.48	4.27	4.39
1985–1989	3.30	3.43	3.06	4.36	3.81	5.27
1990–1994	2.75	2.80	2.69	4.19	3.01	3.81
1995–1999	2.23	2.73	2.39	3.29	2.65	3.54
2000–	1.89	2.06	2.28	2.86	2.47	3.06
Leukemia						
1970–1974	2.86	2.80	2.26	3.28	2.43	3.08
1975–1979	2.50	2.34	1.70	2.53	1.82	1.86
1980–1984	1.79	1.71	1.30	2.17	1.59	1.66
1985–1989	1.50	1.37	1.09	1.51	1.26	1.84
1990–1994	1.20	0.89	0.91	1.47	0.89	1.04
1995–1999	0.88	0.87	0.78	1.07	0.91	1.34
2000–	0.68	0.46	0.69	0.82	0.76	0.90
Lymphomas						
1970–1974	0.33	0.39	–	0.54	0.31	0.27
1975–1979	0.35	0.18	–	0.39	0.27	0.41
1980–1984	0.31	0.23	0.16	0.26	0.22	0.21
1985–1989	0.28	0.22	0.13	0.28	0.14	0.25
1990–1994	0.25	0.12	0.09	0.16	0.09	0.10
1995–1999	0.10	0.09	0.08	0.17	0.09	0.20
2000–	0.06	0.39	0.06	0.18	0.09	0.05
Central nervous system tumors						
1980–1984	0.39	1.01	0.84	1.13	0.93	1.43
1985–1989	0.38	0.88	0.77	0.99	0.98	1.37
1990–1994	0.44	0.75	0.77	0.90	0.88	1.26
1995–1999	0.47	0.84	0.71	0.72	0.74	0.88
2000–	0.42	0.69	0.69	0.78	0.71	1.00
Malignant kidney tumors						
1970–1974	0.20	0.32	0.25	0.44	0.37	0.38
1975–1979	0.11	0.23	0.19	0.33	0.26	0.36
1980–1984	0.12	0.13	0.15	0.27	0.18	0.00
1985–1989	0.07	0.11	0.13	0.18	0.18	0.10
1990–1994	0.07	0.10	0.09	0.18	0.15	0.27
1995–1999	0.05	0.14	0.11	0.11	0.12	0.21
2000–	0.06	0.11	0.10	0.10	0.12	0.11
Malignant bone tumors						
1980–1984	0.17	0.20	0.16	0.26	0.29	0.13
1985–1989	0.16	0.14	0.12	0.27	0.26	0.31
1990–1994	0.12	0.13	0.13	0.23	0.14	0.05
1995–1999	0.14	0.12	0.11	0.16	0.13	0.18
2000–	0.11	0.16	0.11	0.12	0.20	0.25

the main types of childhood cancer. A total of 33 059 childhood cancer deaths were reported in Japan during 1970–2006, of which 353 cancer deaths occurred in 2006. For all cancers combined, the mortality rate during 2000–2006 was 2.20 per 100 000 population for boys and 1.89 for girls. Leukemia was the most common diagnosis. Death rates from leukemia were 0.84 for boys and 0.68 for girls. Mortality from childhood CNS tumors was 0.43 for boys and 0.42 for girls. Geographic variations were observed. The rates of childhood CNS tumor and malignant kidney tumor were lower for both genders in Japan than in other countries.

temporal changes in mortality

Trends of age-standardized mortality from childhood cancer are shown in Figures 1 and 2 and Tables 3 and 4. Mortality for all cancers combined decreased since 1970s in Japan. For boys, a declining trend of 1.58% per year ($P < 0.05$) was observed during 1970–1979, followed by an accelerated decline of 3.78% per year ($P < 0.05$) during 1979–2006. For girls, mortality was high in the 1970s and remained stable in 1996–2006 at a low level, after two significant periods of decline (1972–1995 and 1995–1999). The average annual per cent change (AAPC) in recent 10 years was -3.8% ($P < 0.05\%$) for boys and -1.9% ($P < 0.05$) for girls. In recent 5 years, declining trend only occurred in boys. The average annual per cent change during 2002–2006 was -3.8% ($P < 0.05\%$) for boys, and for girls a nonsignificant decline was observed from 2002 ($\text{AAPC} = -0.6\%$, $P > 0.05$) for girls.

The mortality rate from leukemia in boys remained stable during 1970–1976 ($\text{APC} = -1.10$, $P > 0.05$) and then declined by 4.77% per year ($P < 0.05$) during 1976–2006. For girls, mortality decreased by 4.53% per year ($P < 0.05$) throughout the whole period. The average annual change in recent 10 years was -4.8% ($P < 0.05\%$) for boys and -4.5% ($P < 0.05\%$) for girls. Similar decline trends were also observed in Canada, the United States, Italy, UK (girls) and New Zealand.

In contrast with the dramatic decline in mortality for childhood leukemia, mortality rates from childhood CNS tumor in Japan remained stable at a low level for both genders during 1980–2006. The average annual change in recent 10 years was 0.5% ($P > 0.05$) for boys and 0.0% ($P > 0.05$) for girls. On the contrary, Canada, the United States, UK and New Zealand (girls) showed significant declining trends in the whole period.

With reference to the pattern of mortality for lymphomas, death rates for boys were stable during 1970–1985 and declined significant thereafter by 8.56% per year. The trend for girls leveled off during 1970–1991 and showed a declining trend of 11.85% per year during 1991–2006; however, except for New Zealand females, the death rates in other countries for both genders significantly declined throughout the whole period.

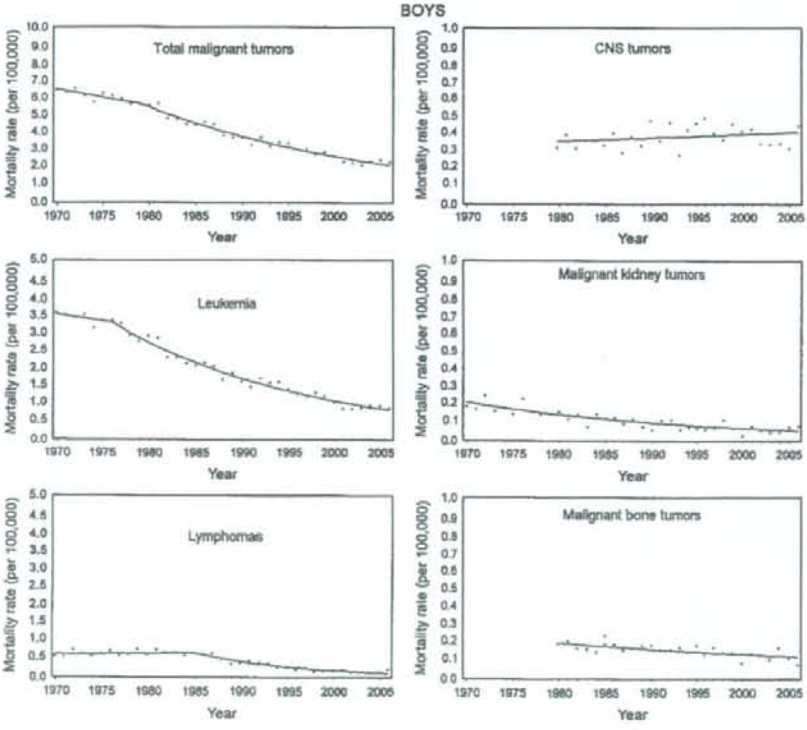

Figure 1. Mortality rates of childhood cancer deaths, boys, Japan, 1970–2006.

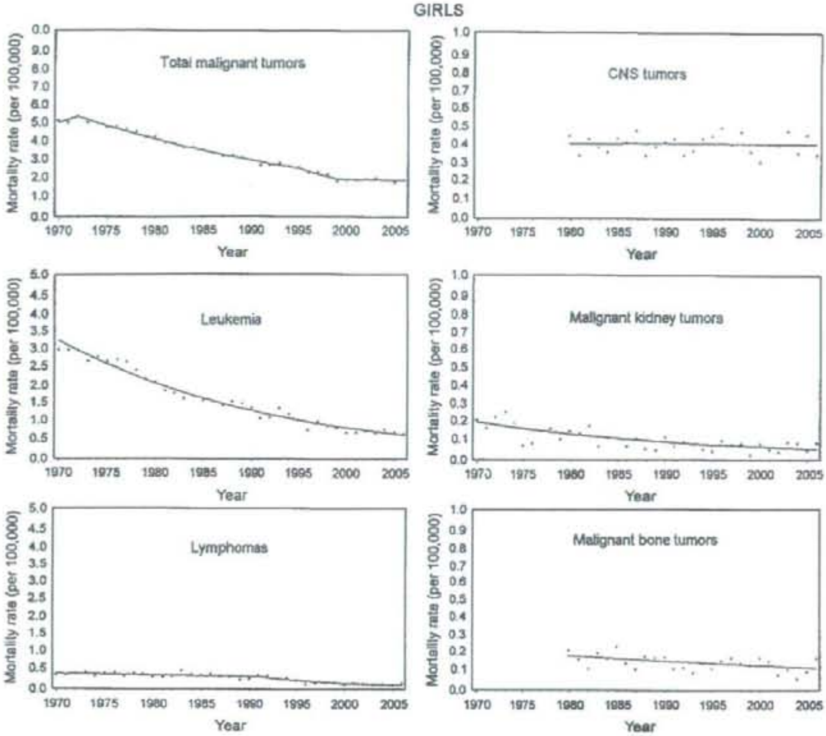

Figure 2. Mortality rates of childhood cancer deaths, girls, Japan, 1970–2006.

Regression analysis also revealed that the death rate for malignant kidney tumors declined by 4.12% per year for boys and 3.98% per year for girls during 1970–2006. Similar trends were observed for malignant bone tumor. Mortality decreased by 2.03% per year for boys and 1.79% per year for girls throughout the whole period.

Mortality rates varied from prefecture to prefecture in Japan. A map of SMR by gender is shown in Figure 3. The SMR was significantly highest among children in Kochi prefecture for boys and Tokushima and Kagoshima prefectures for girls.

discussion

In this study, we quantified the childhood cancer burden in Japan, focusing on mortality, and compared these figures with other developed countries. The results indicated that mortality from childhood cancer in Japan is substantial, while the number of deaths is small. There were 33 059 cases of childhood cancer death over the period 1970–2006 in Japan. Approximately 400 deaths each year were attributed to cancer in children aged 0–14 years. Mortality from all cancers combined in Japan is comparable to that in the European, North American and Oceanic countries included in this study for contrast.

The joinpoint regression method was used in our research to evaluate the trend in childhood cancer deaths. This method has allowed a detailed and accurate description of the pattern of childhood cancer mortality since it identifies the calendar years in which statistically significant changes in trends occurred. This offers a clearer picture of actual trends in mortality over long periods of time rather than using only one trend statistics. We also reported the average annual percentage change in this study. The AAPC can be used to characterize a short segment based on a joinpoint model fit over a much longer series. This is especially advantageous for situations when the data are sparse (e.g. a rare cancer or data from a small geographic area) [7]. Our results showed a declining cancer mortality rate for boys in the whole period and a stable trend for girls in recent 5 years. It is unlikely that the observed time trends in the mortality rate are due to variations in the completeness and accuracy of the population data because the analyzed data were provided by official sources and based on the population census. The significant time trend observed for most tumor types is congruent with improvements in diagnosis, therapy and supportive care.

The dramatic decrease in mortality observed for childhood leukemia, which accounts for ~50% of all childhood cancer

Table 3. The APC of childhood cancer mortality rates (boys)

Country	Trend 1		Trend 2		Trend 3		Trend 4		AAPC	
	Years	APC	Years	APC	Years	APC	Years	APC	Last 10 observations	Last 5 observations
Total malignant tumors										
Japan	1970–1979	−1.58*	1979–2006	−3.78*					−3.8*	−3.8*
Canada	1970–2004	−3.64*							−3.6*	−3.6*
United States	1970–1998	−3.22*	1998–2005	−0.26					−0.3	−0.9
Italy	1970–1985	−2.32*	1985–1989	−8.69	1989–1993	6.96	1993–2003	−5.89*	−5.9*	−5.9*
UK	1970–2005	−2.93*							−2.9*	−2.9*
New Zealand	1970–2004	−2.50*							−2.5*	−2.5*
Leukemia										
Japan	1970–1976	−1.10	1976–2006	−4.77*					−4.8*	−4.8*
Canada	1970–2004	−5.00*							−5.0*	−5.0*
United States	1970–1984	−4.95*	1984–2005	−3.39*					−3.4*	−3.4*
Italy	1970–2003	−3.69*							−3.7*	−3.7*
UK	1970–2005	−3.74*	2003–2005	−27.41					−9.6	−16.4
New Zealand	1970–1997	−2.12*	1997–2004	−18.03*					−14.7*	−18.0*
Lymphomas										
Japan	1970–1985	0.39	1985–2006	−8.56*					−8.6*	−8.6*
Canada	1970–2004	−6.10*							−6.1*	−6.1*
United States	1980–2005	−5.63*							−5.6*	−5.6*
Italy	1970–2003	−4.46*							−4.5*	−4.5*
UK	1970–2005	−4.56*							−4.6*	−4.6*
New Zealand	1970–2004	−2.57*							−2.6*	−2.6*
Central nervous system tumors										
Japan	1980–2006	0.48							0.5	0.5
Canada	1980–2004	−2.13*							−2.1*	−2.1*
United States	1980–2005	−1.07*							−1.1*	−1.1*
Italy	1980–2003	−2.19*							−2.2*	−2.2*
UK	1980–2005	−1.25*							−1.2*	−1.2*
New Zealand	1980–2004	−0.86							−0.9	−0.9
Malignant kidney tumors										
Japan	1970–2006	−4.12*							−4.1*	−4.1*
Canada	1970–1996	−7.91*	1996–2004	17.70*					14.5*	17.7*
United States	1970–1987	−5.46*	1987–2005	−1.73*					−1.7*	−1.7*
Italy	1970–2003	−4.91*							−4.9*	−4.9*
UK	1970–2005	−3.64*							−3.6*	−3.6*
New Zealand	1970–2004	−1.99							−2.0*	−2.0*
Malignant bone tumors										
Japan	1980–2006	−2.03*							−2.0*	−2.0*
Canada	1980–2004	−2.32*							−2.3*	−2.3*
United States	1980–1990	−4.41*	1990–2005	1.31					1.3	1.3
Italy	1980–2003	−4.43*							−4.4*	−4.4*
UK	1980–2005	−2.93*							−2.9*	−2.9*
New Zealand	1980–2004	−0.23							−0.2	−0.2

*$P < 0.05$.

APC is the annual per cent change; AAPC is average annual per cent change.

deaths, is consistent with improvements in survival, particularly for patients with acute lymphoblastic leukemia. This increase in survival is due to more effective antileukemic therapy, such as multidrug chemotherapy protocols, with a reduction in the number of relapses and resistant disease, but also due to improvements in supportive care, such as antibiotics, antifungal treatment, blood banking, transplant procedures and pediatric intensive care. In fact, the 5-year survival rate of acute lymphoblastic leukemia increased from 20% to 30% in the 1960s to 60% to 75% in the 1980s in developed countries. Current survival rates are ∼80% for acute lymphoblastic leukemia (ALL) [8] and 50%–70% for acute myelogenous leukemia. In Japan, a population-based study in Osaka prefecture indicated that the 5-year survival rate of childhood leukemia increased from 32.4% in 1975–1984 to 60.4 in 1985–1994 [1]. National incidence trends could not be